© 2019. Published by The Company of Biologists Ltd | Biology Open (2019) 8, bio040683. doi:10.1242/bio.040683

RESEARCH ARTICLE

# Fgf3 is crucial for the generation of monoaminergic cerebrospinal fluid contacting cells in zebrafish

**Isabel Reuter[1,2], Jana Jäckels[2], Susanne Kneitz[2], Jochen Kuper[3], Klaus-Peter Lesch[1,4] and Christina Lillesaar[2,5,*]**

## ABSTRACT

In most vertebrates, including zebrafish, the hypothalamic serotonergic cerebrospinal fluid-contacting (CSF-c) cells constitute a prominent population. In contrast to the hindbrain serotonergic neurons, little is known about the development and function of these cells. Here, we identify fibroblast growth factor (Fgf)3 as the main Fgf ligand controlling the ontogeny of serotonergic CSF-c cells. We show that *fgf3* positively regulates the number of serotonergic CSF-c cells, as well as a subset of dopaminergic and neuroendocrine cells in the posterior hypothalamus via control of proliferation and cell survival. Further, expression of the ETS-domain transcription factor *etv5b* is downregulated after *fgf3* impairment. Previous findings identified *etv5b* as critical for the proliferation of serotonergic progenitors in the hypothalamus, and therefore we now suggest that Fgf3 acts via *etv5b* during early development to ultimately control the number of mature serotonergic CSF-c cells. Moreover, our analysis of the developing hypothalamic transcriptome shows that the expression of *fgf3* is upregulated upon *fgf3* loss-of-function, suggesting activation of a self-compensatory mechanism. Together, these results highlight Fgf3 in a novel context as part of a signalling pathway of critical importance for hypothalamic development.

**KEY WORDS: Fgf-signalling, Serotonin, Dopamine, Hypothalamus, Central nervous system**

## INTRODUCTION

Serotonin (5-hydroxytryptamine, 5-HT) is an ancient signalling molecule present in the nervous system of animals from cnidarian and bilaterian lineages (Hay-Schmidt, 2000; Kass-Simon and Pierobon, 2007; Moroz and Kohn, 2016; Stach, 2005). Accordingly, 5-HT modulates a variety of physiological processes and behaviours in most animals (e.g. Curran and Chalasani, 2012; Fossat et al., 2014; Gillette, 2006; Lucki, 1998; Trowbridge et al., 2011). In placental mammals, serotonergic neurons are, with a few potential exceptions (Ballion et al., 2002; Ugrumov et al., 1989), uniquely located in the raphe nuclei of the hindbrain (Deneris and Gaspar, 2018). In contrast, additional serotonergic cell populations are found in the forebrain and spinal cord in cartilaginous and bony fish, amphibians, reptiles, birds and monotremes (Lillesaar, 2011; Montgomery et al., 2016). Most of these non-raphe cell populations are truly serotonergic as they contain not only 5-HT, but also proteins required for 5-HT metabolism, packaging and transport. To what extent the development of different populations of serotonergic cells is controlled by the same paracrine signals and gene regulatory networks to ultimately express the mature serotonergic phenotype (i.e. capacity to synthesise 5-HT) is still unclear.

The ontogeny as well as the regulatory transcriptional networks of raphe serotonergic neurons are well described (Deneris and Gaspar, 2018; Deneris and Wyler, 2012; Flames and Hobert, 2011; Kiyasova and Gaspar, 2011; Lillesaar et al., 2007, 2009; McLean and Fetcho, 2004; Norton et al., 2005; Teraoka et al., 2004). In contrast, little is known about the development of the remaining populations in the central nervous system. In zebrafish, the hypothalamus contains by far the highest number of serotonergic cells (Lillesaar, 2011). These cells are small, bipolar cells with one thick process contacting the ventricle suggesting that they can communicate over longer distances via the cerebrospinal fluid (CSF), and the other process projecting locally in the brain (Lillesaar, 2011; Sano et al., 1983; Vígh et al., 2004). Anatomically, these cells are further separated into three clusters in teleost fish; the anterior, intermediate (i.) and posterior (p.) paraventricular organ clusters (Ekström et al., 1985; Kaslin and Panula, 2001), of which the latter is located around the posterior recess, a ventricular structure found in the hypothalamus of teleosts (Xavier et al., 2017). Overlapping expression of *tph1a*, *slc6a4b*, *ddc*, *mao* and *vmat2* (Anichtchik et al., 2006; Lillesaar et al., 2007; Norton et al., 2008; Sallinen et al., 2009; Yamamoto et al., 2011) shows an active 5-HT metabolism in the region. Notably, serotonergic and dopaminergic cells are largely intermingled populations in the hypothalamus (Filippi et al., 2009; Kaslin and Panula, 2001; McLean and Fetcho, 2004; Xavier et al., 2017; Yamamoto et al., 2010, 2011).

Progenitors giving rise to neuronal and glial precursors of the developing hypothalamus are located at the ventricular zone (Duncan et al., 2016; Xie and Dorsky, 2017). Eventually the progenitors exit the cell cycle, migrate laterally and continue differentiation. Lineage specific combinations of transcription factors control the fate of the precursors (Biran et al., 2015; Burbridge et al., 2016; Muthu et al., 2016; Ware et al., 2014; Xie and Dorsky, 2017). The precise set of paracrine molecules and transcription factors required in time and space for each cell type is still a matter of investigation, as is the extent of evolutionary conservation. In zebrafish, the location of the serotonergic cells in

[1]Division of Molecular Psychiatry, Center of Mental Health, University of Würzburg, Germany. [2]Department of Physiological Chemistry, Biocenter, Am Hubland, University of Würzburg, Germany. [3]Structural Biology, Rudolf Virchow Center for Biomedical Research, University of Würzburg, Germany. [4]Laboratory of Psychiatric Neurobiology, Institute of Molecular Medicine, I.M. Sechenov First Moscow State Medical University, Moscow, Russia; Department of Neuroscience, School for Mental Health and Neuroscience (MHeNS), Maastricht University, Maastricht, The Netherlands. [5]Department of Child and Adolescent Psychiatry, Psychosomatics and Psychotherapy, Center of Mental Health, University Hospital of Würzburg, Germany.

*Author for correspondence (christina.lillesaar@biozentrum.uni-wuerzburg.de)

K.-P.L., 0000-0001-8348-153X; C.L., 0000-0002-5166-2851



**Received 29 November 2018; Accepted 23 April 2019**

Biology Open (2019) 8, bio040683. doi:10.1242/bio.040683

the posterior hypothalamus suggests that their fate is favoured by posteriorising signals such as Wnt and Fgf (Kapsimali et al., 2004; Xie and Dorsky, 2017), and inhibited by anteriorising signals such as late Shh expression (Mathieu et al., 2002; Muthu et al., 2016). Indeed, Fgf ligands, receptors and downstream targets are expressed in the posterior zebrafish hypothalamus (Bosco et al., 2013; Herzog et al., 2004; Jackman et al., 2004; Liu et al., 2013; Reifers et al., 1998; Topp et al., 2008). Similarly to raphe serotonergic neurons, hypothalamic serotonergic CSF-c cells along with dopaminergic cells depend on Fgf-signalling during development (Bosco et al., 2013; Koch et al., 2014; Teraoka et al., 2004). Furthermore, Etv5b, a member of the ETS-domain transcription factor family that is a direct downstream target of Fgf-signalling (Ornitz and Itoh, 2015; Raible and Brand, 2001; Roussigné and Blader, 2006), regulates the proliferation of serotonergic progenitors (Bosco et al., 2013).

Here, we are focusing on the hypothalamic serotonergic cells of zebrafish, a frequently used model organism in biomedical research. Using three different approaches for genetic manipulation, we identify Fgf3 as the main Fgf ligand critical for development of serotonergic as well as dopaminergic CSF-c cells and *arginine vasopressin* (*avp*)-expressing cells located in the posterior hypothalamus. Further, based on sequencing of the transcriptome of microdissected hypothalami we identify genes belonging to the Fgf-signalling pathway that are expressed in the developing hypothalamus, and demonstrate mild alterations of Fgf-signalling after impairment of *fgf3*. With this information we acquire a better knowledge about the signalling networks promoting the ontogeny of central serotonergic cells.

## RESULTS

### *fgf3* is expressed in the developing hypothalamus and spatially correlates with the location of putative serotonergic CSF-c cells

Among the described Fgf ligands, *fgf3* exhibits the most prominent distribution in the posterior hypothalamus (Herzog et al., 2004; Jackman et al., 2004; Liu et al., 2013; Reifers et al., 1998; Topp et al., 2008) presumably where serotonergic precursor cells are located, therefore rendering Fgf3 a likely candidate regulating the development of hypothalamic serotonergic CSF-c cells. To explore the dynamics of hypothalamic *fgf3* expression we performed a spatio-temporal expression analysis. We could confirm presence of *fgf3* transcripts in the developing hypothalamus (Fig. 1). More specifically, transcripts were first detectable at 20 somites in the hypothalamic primordium (Fig. 1A–D). This expression was maintained until 30 h post fertilisation (hpf) (Fig. 1E,F). From 36 hpf and onwards the signal was restricted to the posterior

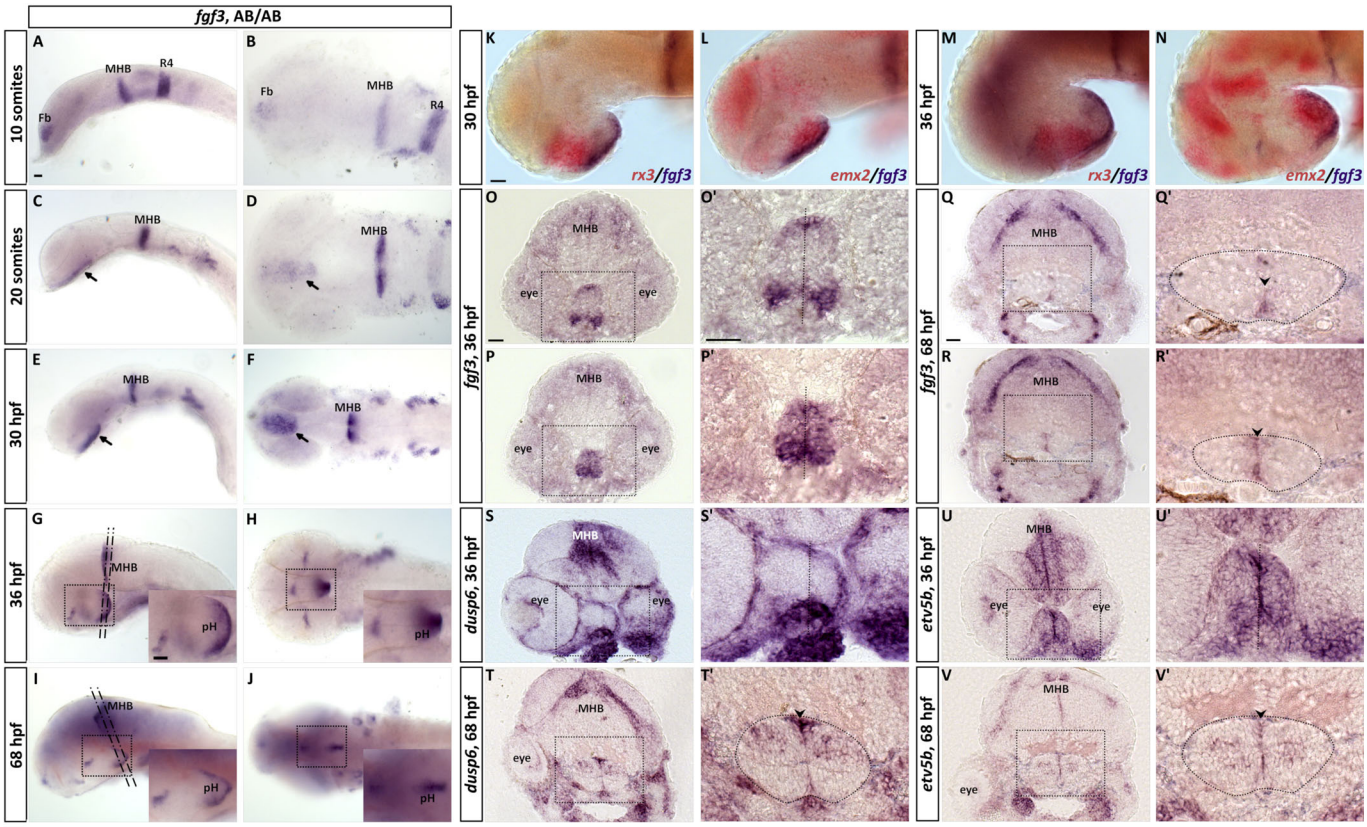


**Fig. 1. RNA *in situ* hybridisation reveals *fgf3* expression in the developing hypothalamus.** (A,B) At 10 somites, *fgf3* transcripts are detectable in the forebrain (Fb), at the mid- hindbrain boundary (MHB) and in rhombomere 4 (R4). (C–F) At 20 somites and 30 hpf, *fgf3* expression is present in the hypothalamic primordium (arrows), and (G–J) at 36 and 68 hpf in the posterior hypothalamus (pH). Left column depicts lateral views and right column ventral views. Insets are high magnifications of boxed areas. Anterior to the left. (K–N) Double *in situ* hybridisation for *fgf3* with *rx3* or *emx2* at 30 and 36 hpf shows that *fgf3* is concentrated to the posterior hypothalamus. Anterior to the left. (O–V) 20 µm frontal cryosections at levels indicated in G and I of embryos hybridised for *fgf3*, *dusp6* and *etv5b* at 36 or 68 hpf. O′–V′ are high magnifications of boxed areas. Dashed lines in O′, P′, S′ and U′, and arrowheads in T′, Q′, R′ and V′ indicate ventricle. Dashed circles in T′, Q′, R′ and V′ outline borders of posterior hypothalamus. At 36 hpf, expression of *fgf3* spans the entire medial to lateral dimension of the posterior hypothalamus. *dusp6* and *etv5b* are similarly broadly expressed. At 68 hpf, the expression of *fgf3* is restricted to cells located medially at the ventricle (arrowheads), while *dusp6* and *etv5b* are present laterally, in cells around the posterior recess. Scale bars: 30 µm.

Biology Open (2019) 8, bio040683. doi:10.1242/bio.040683

hypothalamus (Fig. 1G,H,O,P) partly overlapping with *emx2*, but not *rx3* expression (Fig. 1K–N). Gradually *fgf3* expression got limited to cells located medially along the third ventricle at 68 hpf (Fig. 1I,J,Q,R). In parallel, transcripts for known Fgf targets, such as *dusp6* and *etv5b*, showed a broad distribution in the posterior hypothalamus at 36 hpf, but were more restricted at 68 hpf (Fig. 1S–V). In contrast to *fgf3*, however, *dusp6* and *etv5b* were not limited to the medial ventricular expression, but also included cells laterally in the parenchyme surrounding the posterior recess. Our expression analysis, thus, strengthens the hypothesised role of Fgf3 as an important regulator during the ontogeny of hypothalamic serotonergic cells. Notably, *fgf3* expression precedes the expression of *tph1a* and 5-HT by several hours (Bellipanni et al., 2002; Bosco et al., 2013) arguing for an early effect on progenitors and possibly differentiation.

### Fgf3 regulates *etv5b* expression in the posterior hypothalamus

The transcription factor Etv5b is a downstream target of Fgf-signalling in various contexts (Mason, 2007; Ornitz and Itoh, 2015; Raible and Brand, 2001; Roehl and Nüsslein-Volhard, 2001; Roussigné and Blader, 2006). However, the identity of the Fgf(s) regulating *etv5b* and thereby the ontogeny of hypothalamic serotonergic populations remains unknown. Preliminary observations from Bosco et al. (2013) and our current *fgf3* expression analysis (see above), suggest that Fgf3 might be the main Fgf-ligand in this context. To explore this hypothesis, we investigated hypothalamic *etv5b* expression in the *fgf3* mutant, *fgf3*$^{t24152}$, which was suggested to be a null mutant (amorph) (Herzog et al., 2004), as well as in *fgf3* morphants. Our analysis revealed a reduced expression of *etv5b* in mutants compared to wild-type siblings at 36 hpf (Fig. 2A–C). Further, *etv5b* expression was reduced in a dose-dependent manner as the *in situ* hybridisation signal was weaker in homozygotes than in heterozygotes. Our RNA sequencing data supported these observations by revealing fewer *etv5b* transcripts in homozygous *fgf3*$^{t24152}$ mutants than in wild types at 3 and 7 days post fertilisation (dpf) (Fig. 2F), although the read count values did not pass our defined thresholds. Similarly we observed a reduction of *etv5b* expression in *fgf3* morphants compared to controls (Fig. 2D,E). However, the *etv5b* signal was never completely abolished, neither in our *in situ* hybridisation nor in our RNA sequencing experiments. Thus, we show that Fgf3 regulates *etv5b* expression in the developing posterior hypothalamus.

### Fgf3 impacts on monoaminergic cell development in posterior hypothalamus

After identifying Fgf3 as a possible regulator of hypothalamic serotonergic CSF-c cell development based on expression data, we next tested this hypothesis functionally. For this, we applied three complementary strategies to manipulate *fgf3* activity. Firstly, we used the *fgf3*$^{t24152}$ mutant, which has a G to A transition point mutation resulting in a premature stop codon and, thereby, a truncated Fgf3 protein with 69.1% of the wild-type amino acid sequence remaining (Fig. S1D) (Herzog et al., 2004). Secondly, we created a *fgf3* morpholino knockdown, which leads to a truncated protein containing 49.6% of the wild-type amino acid sequence (Fig. S1D). Finally, we applied CRISPR/Cas9 to generate indel mutations causing either a nonsense amino acid sequence or a premature stop close to the N-terminal (Fig. S2). All embryos with a manipulated *fgf3*, irrespective of the used strategy, showed similar defects in ear and craniofacial development at 72 hpf (Fig. S3). Embryos exhibited fused otoliths presumably due to a role of Fgf3 in anterior ear specification, and malformations of the ventral head skeleton attributed to the loss of ceratobranchial cartilage (Hammond and Whitfield, 2011; Herzog et al., 2004). Additionally, embryos with manipulated *fgf3* displayed a defect in swim bladder development or inflation (not shown). The fact that we could confirm these phenotypes in homozygous *fgf3*$^{t24152}$ mutants and reproduce similar defects in *fgf3* morpholino and CRISPR/Cas9-injected embryos show that all three approaches to manipulate *fgf3* produce qualitatively comparable results. Apart

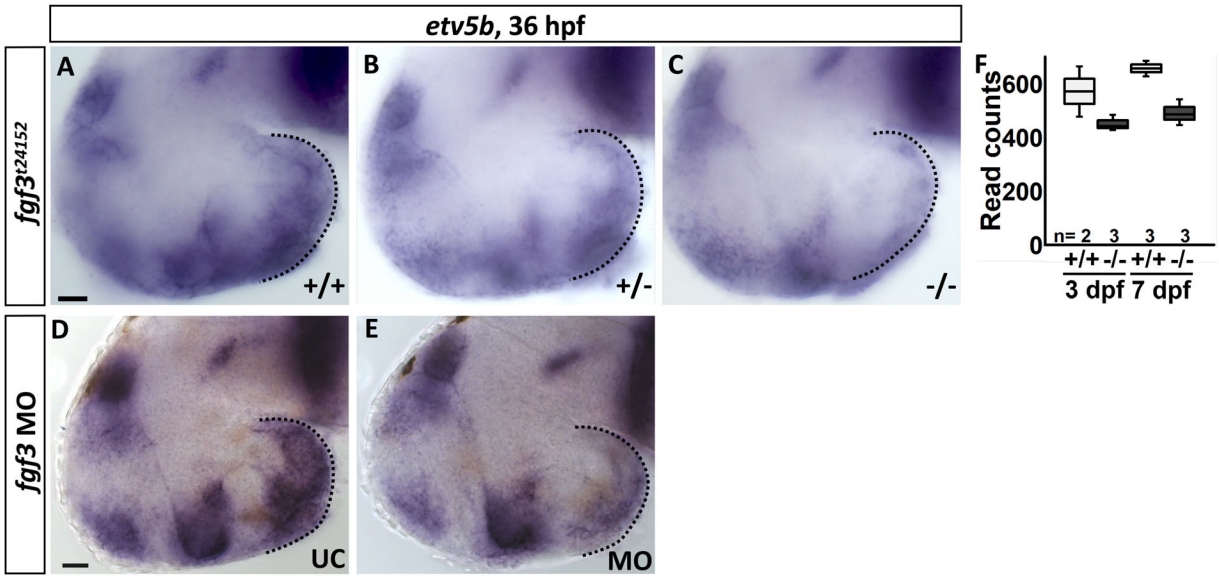


**Fig. 2. *fgf3*$^{t24152}$ mutants and *fgf3* morphants exhibit a reduced expression of *etv5b* in the posterior hypothalamus.** (A–E) Light microscopic pictures of wild type (+/+), heterozygous (+/–) and homozygous (–/–) *fgf3*$^{t24152}$ mutant siblings, and uninjected control (UC) and *fgf3* morphant (MO) siblings processed for RNA *in situ* hybridisation for *etv5b* at 36 hpf. Dotted line indicates posterior hypothalamus where *etv5b* is expressed. Notably, the hypothalamic *etv5b* expression is weaker in +/– than in +/+ embryos, and strongly reduced in –/– embryos. Similarly, *etv5b* expression is weaker in MO embryos than in UC embryos. Lateral views, anterior to the left. Scale bars: 30 µm. (F) Read counts of *etv5b* obtained by RNA sequencing of dissected hypothalami of +/+ and *fgf3*$^{t24152}$ –/– mutants at 3 and 7 dpf. Tukey boxplots show median, 25–75% percentile, IQR whiskers and outliers. *n*=number of analysed replicates.

Biology Open (2019) 8, bio040683. doi:10.1242/bio.040683

from the described defects, no severe morphological abnormalities or increased overall cell death were observed (Figs S3, S4, S6J). Next, we focused on the impact on hypothalamic serotonergic CSF-c cell development, applying all three strategies in parallel. The number of hypothalamic 5-HT immunoreactive cells in the intermediate (i.) and posterior (p.) populations were quantified at 72 hpf, a stage when the maturation of the serotonergic cells is well on the way (Bellipanni et al., 2002; Bosco et al., 2013; McLean and Fetcho, 2004). In addition, to label catecholaminergic cells, 3 dpf embryos were co-stained with a TH1 antibody, and 4 dpf embryos were processed for *in situ* hybridisation for *th2* (Chen et al., 2009). TH1-positive cells of the posterior tuberculum/hypothalamus are subdivided into several subpopulations (Rink and Wullimann, 2002). We quantified the TH1 immunoreactive CSF-c cells in regions DC 4/5/6 and TH1 and *th2* expressing cells in DC 7, which are dopaminergic (Filippi et al., 2009; Yamamoto et al., 2010, 2011, but see Xavier et al., 2017). Region DC 4/5/6 is located close to the i. serotonergic population while DC 7 cells are intermingled with the p. serotonergic population (Kaslin and Panula, 2001; McLean and Fetcho, 2004).

We found that homozygous *fgf3*$^{t24152}$ mutants, *fgf3* morpholino and CRISPR/Cas9-injected embryos had reduced numbers of serotonergic CSF-c cells, but depending on the approach used the severity of the phenotype varied (Fig. 3). Specifically, homozygous *fgf3*$^{t24152}$ mutants had 17% fewer serotonergic CSF-c cells than wild-type siblings (Fig. 3Q, Table S3), *fgf3* morphants had a reduction of 45% compared to controls (Fig. 3T, Table S3), and CRISPR/Cas9-injected embryos had 49% fewer serotonergic CSF-c cells than uninjected controls and 42% fewer than control siblings injected with Cas9 only (Fig. 3W, Table S3). The reduction of i./p. serotonergic CSF-c cells persisted at 4 dpf in *fgf3* morphants with a loss of 33% (Fig. S5, Table S3).

With respect to the TH1 immunoreactive cells, the numbers in DC 4/5/6 were never significantly affected after any of the *fgf3* manipulations (Fig. 3R,U,X, Fig. S5, Table S3). In contrast, homozygous *fgf3*$^{t24152}$ mutants, *fgf3* morpholino and CRISPR/Cas9-injected embryos had fewer cells in DC 7 (Fig. 3). A reduction of TH1-positive cells by 32% was detectable in homozygous *fgf3*$^{t24152}$ mutants compared to wild-type siblings (Fig. 3S, Table S3). Further, homozygous *fgf3*$^{t24152}$ mutants had 38% fewer TH1-positive cells than heterozygotes. In *fgf3* morphants, the number of TH1-expressing cells in DC7 was reduced by 70% compared to uninjected controls (Fig. 3V, Table S3). CRISPR/Cas9-injected embryos had 35% fewer TH1-positive cells in comparison to uninjected controls, and 44% fewer compared to controls injected with Cas9 only (Fig. 3Y, Table S3). The reduction of TH1-positive DC 7 cells persisted at 4 dpf in *fgf3* morphants with a loss of 34% (Fig. S5, Table S3). Similarly, the number of *th2* expressing cells was reduced by 33% in morphants compared to controls (Fig. S5L–N, Table S3).

Taken together, using three independent techniques to manipulate *fgf3* activity, we demonstrated a consistent loss of monoaminergic CSF-c cells after *fgf3* impairment, showing a developmental dependency of these cells on Fgf3. Interestingly, this seemed to specifically affect the populations in the posterior hypothalamus.

### *oxytocin* (*oxt*) and *cortistatin* (*cort*) expressing neuroendocrine cells are unaffected by impaired *fgf3* function

To test the specific dependence of the monoaminergic CSF-c cells in the posterior hypothalamus on Fgf3, three additional cell populations, including neuroendocrine cells expressing *oxytocin* (*oxt*), *arginine vasopressin* (*avp*) and *cortistatin* (*cort*) were investigated (Devos et al., 2002; Eaton et al., 2008; Unger and Glasgow, 2003). These populations were chosen due to their spatial proximity to the hypothalamic monoaminergic regions. *fgf3*$^{t24152}$ mutants and *fgf3* morphants were labelled for *oxt*, *avp* and *cort* at 72 hpf, and the number of positive cells was counted. The *oxt* and *cort* cell numbers were not decreased in hetero- and homozygous *fgf3*$^{t24152}$ mutants or *fgf3* morphants (Fig. 4, Table S3) compared to control siblings. However, there was a significant reduction in the number of *avp*-positive cells (Fig. 4E–H, Table S3). Homozygous *fgf3*$^{t24152}$ mutants lost 16% of the cells compared to wild types and 14% compared to heterozygotes (Fig. 4O, Table S3). In *fgf3* morphants, *avp*-expressing cell numbers decreased by 11% compared to controls (Fig. 4P, Table S3). Thus, *avp*-expressing, but not *oxt*- or *cort*-expressing cells showed dependency on Fgf3. Interestingly, the most posteriorly located *avp*-positive cells were more affected than anteriorly located cells in mutants and morphants (Fig. 4F,H), and therefore mirroring the effects on the TH1-positive cells.

### *fgf3*$^{t24152}$ mutants and *fgf3* morphants have a smaller hypothalamus

To determine whether the loss of hypothalamic monoaminergic CSF-c cells, as well as *avp*-expressing cells consequently resulted in a smaller hypothalamus, we measured the size of the hypothalamic domain in *fgf3*$^{t24152}$ mutants and *fgf3* morphants. *nkx2.4b* expression at 36, 48 and 72 hpf was used to visualise the hypothalamic domain, which was subsequently measured in a semi-automatic manner (Fig. 5, Fig. S6). Qualitatively, neither the ventral nor the lateral silhouette of the *nkx2.4b* domain showed any major alterations after *fgf3* impairment suggesting that the gross organisation of the domain is similar (Fig. 5, Fig. S6). However, we noticed a difference in size, which was more prominent from a ventral view compared to the lateral view. This notion can be explained by a developmental change in 3D shape of the domain going from a largely oval 'egg'-shape at 36 hpf to a broader and flatter shape at 72 hpf, in particular at the lateral edges of the posterior end surrounding the posterior recess (Fig. S6K). The posterior hypothalamic end houses the prominent posterior serotonergic and DC7 dopaminergic populations, and a loss of those cells will consequently result in a smaller ventral silhouette. Concentrating on the ventral view, homozygous *fgf3*$^{t24152}$ mutants showed a trend (6%) towards a smaller hypothalamic domain at 36 hpf (Fig. 5M, Table S3). At 48 hpf a significant reduction of 11% in homozygous *fgf3*$^{t24152}$ mutants compared to wild-type siblings was recorded, and at 72 hpf the hypothalamus was smaller in homozygous *fgf3*$^{t24152}$ mutants compared to both heterozygous mutant (10%) and wild-type (14%) siblings (Fig. 5O,Q, Table S3). As expected, measurements of *fgf3* morphants revealed significantly reduced hypothalamic size, but the body length was unchanged (Fig. 5, Fig. S6J). At 36 hpf the *nkx2.4b*-positive domain in *fgf3* morphants was 19% smaller compared to uninjected controls (Fig. 5N, Fig. S6, Table S3). Further, at 48 and 72 hpf, the reduction was 16% and 15%, respectively (Fig. 5P,R, Table S3). Thus, we noticed that the size of the hypothalamic domain was more reduced in *fgf3* morphants than in *fgf3*$^{t24152}$ mutants at all stages examined, which was in line with the stronger monoaminergic phenotypes observed in *fgf3* morphants compared to *fgf3*$^{t24152}$ mutants described above.

### Fgf3 regulates proliferation and survival in the developing posterior hypothalamus

*fgf3* expression precedes the expression of *tph1a* and 5-HT by several hours (Bellipanni et al., 2002; Bosco et al., 2013). Further, in this study we noticed a reduction of hypothalamic size already, before the appearance of mature monoaminergic cells. Together these

Biology Open (2019) 8, bio040683. doi:10.1242/bio.040683

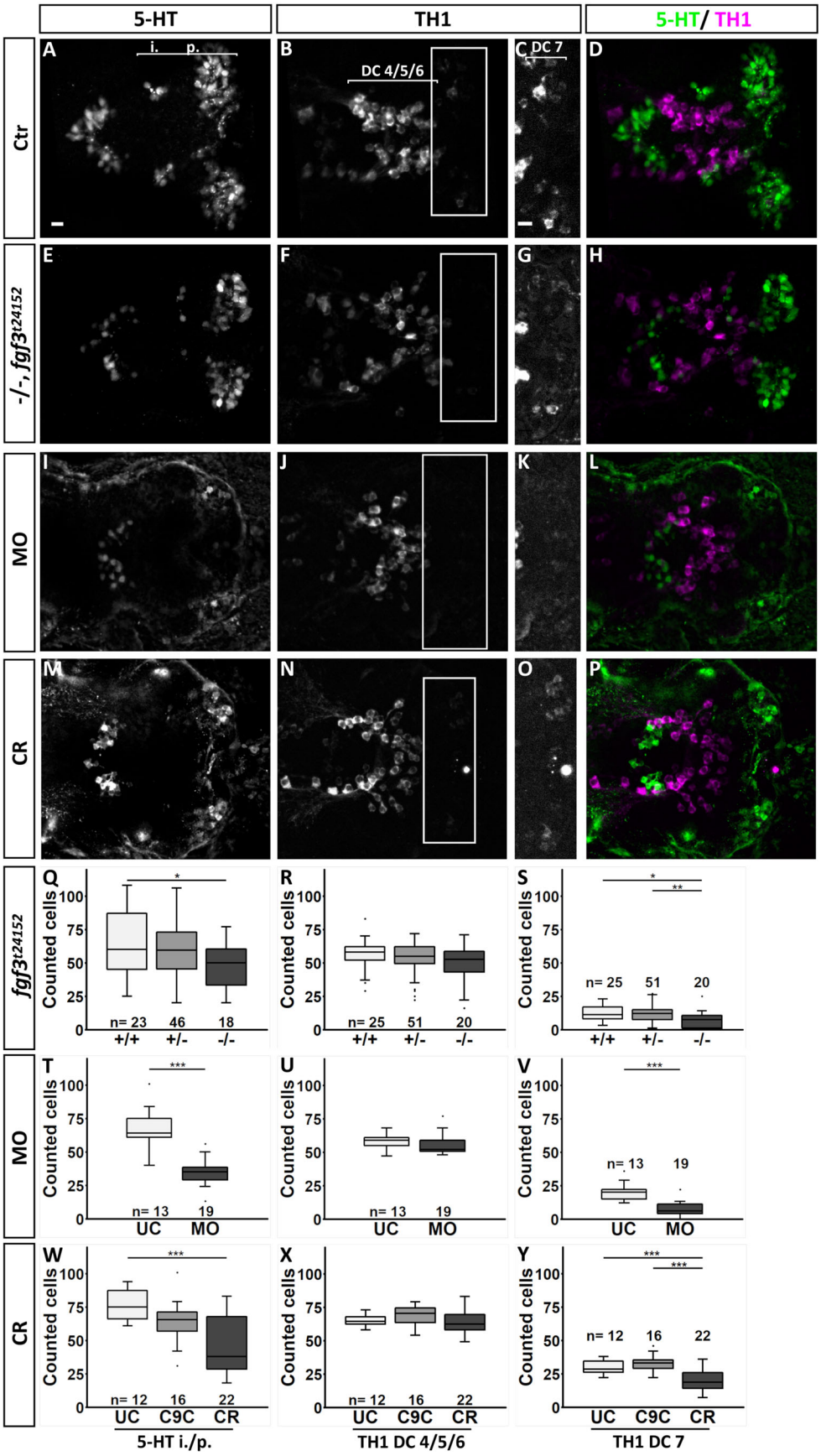


**Fig. 3. Quantification of the number of serotonergic cells in the intermediate (i.)/posterior (p.) clusters and of dopaminergic cells in the DC 4/5/6 and DC 7 clusters in the hypothalamus at 72 hpf after *fgf3* impairment.** (A–P) Confocal maximum intensity projections from wild-type controls (Ctr), homozygous *fgf3*$^{t24152}$ mutants (–/–), *fgf3* morphants (MO) or *fgf3* CRISPR/Cas9-injected embryos (CR) immunostained for 5-HT (green) and TH1 (magenta) shown as single channels and merged. C,G,K and O show boxed areas in B,F,J and N, respectively, with adjusted brightness and contrast to reveal faint TH1 immunoreactive cells of the DC 7 cluster. Ventral views, anterior to the left. Scale bars: 10 µm. (Q–Y) Quantifications of 5-HT and TH1 positive cells after *fgf3* impairment and in control siblings. The number of serotonergic cells was counted in the i./p. clusters as indicated by the line in A. The number of dopaminergic cells was counted in the DC 4/5/6 and DC 7 clusters as indicated by the lines in B and C. Tukey boxplots show median, 25–75% percentile, IQR whiskers and outliers. *n*=number of analysed individuals. +/–, heterozygous *fgf3*$^{t24152}$ mutants; UC, uninjected siblings; C9C, injected with Cas9 only. **P*>0.05, ***P*>0.01, ****P*>0.001.

Biology Open (2019) 8, bio040683. doi:10.1242/bio.040683

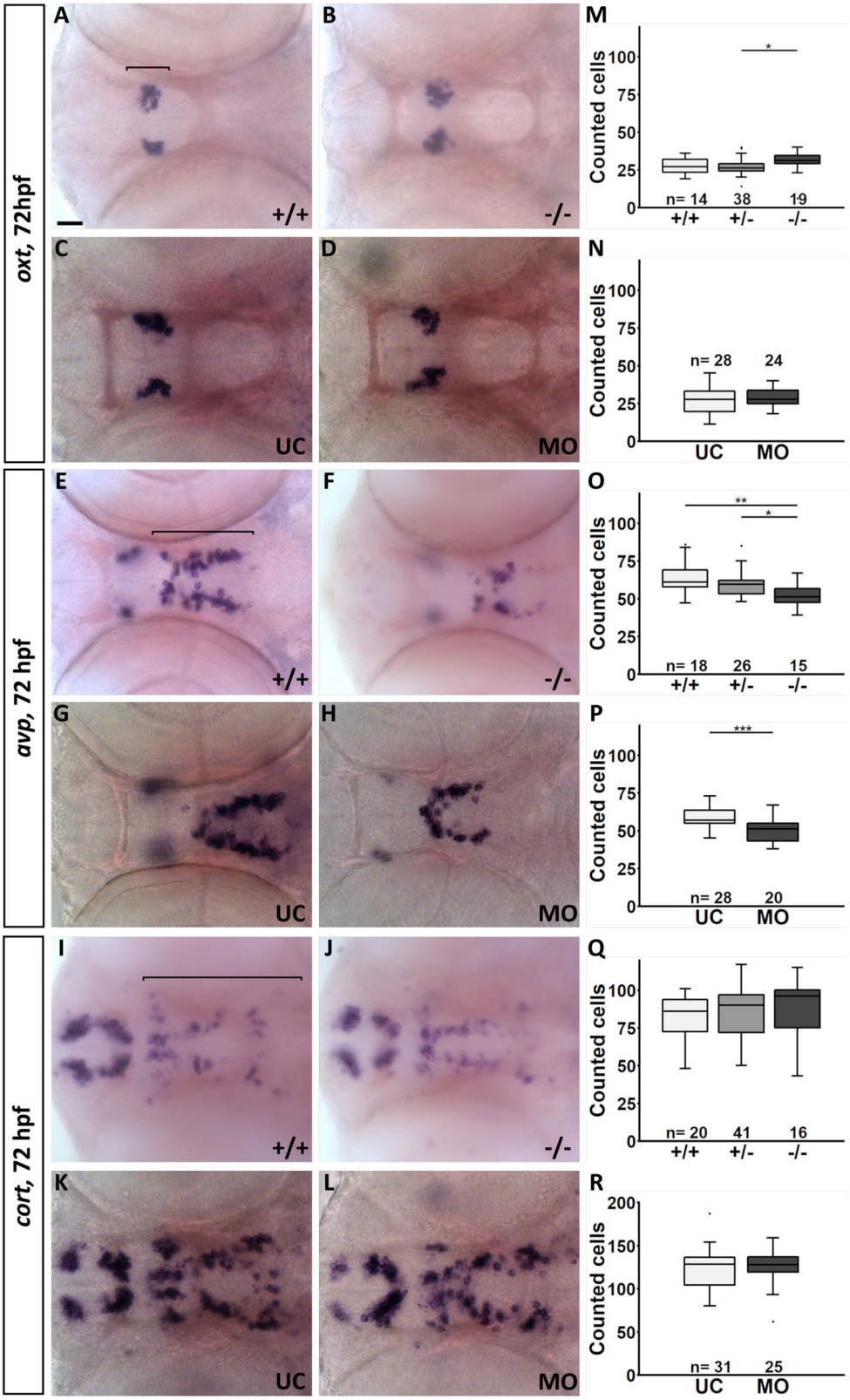


**Fig. 4. Quantification of the number of *oxt*-, *avp*- and *cort*-expressing cells in the hypothalamus of *fgf3*$^{t24152}$ mutants and *fgf3* morphants at 72 hpf.** (A–L) Light microscopic pictures of wild type (+/+) and homozygous *fgf3*$^{t24152}$ mutant (–/–) siblings as well as *fgf3* morphants (MO) and uninjected control siblings (UC) processed for RNA *in situ* hybridisation. The posterior cells expressing *avp* are more affected by impaired *fgf3* than the anterior ones. Ventral views, anterior to the left. Scale bar: 30 µm. (M–R) Quantifications of *oxt*-, *avp*- and *cort*-positive cells in *fgf3*$^{t24152}$ mutants, *fgf3* morphants and control siblings. Cell clusters used for the analyses are indicated by the lines in A, E and I. Tukey boxplots show median, 25–75% percentile, IQR whiskers and outliers. *n*=number of analysed individuals, +/–, heterozygous *fgf3*$^{t24152}$ mutants. **P*>0.05, ***P*>0.01, ****P*>0.001.

observations argue for an early effect of *fgf3* on progenitors later giving rise to mature monoaminergic cells. To test for this possibility we analysed proliferation rate and cell death at 36 hpf in the posterior hypothalamus after impairment of *fgf3* (Fig. 6, Table S3). Using 5-bromo-2′-deoxyuridine (BrdU) and phospho-histone H3 (phH3) we labelled cells in S-phase and M-phase, respectively. We noticed a significant reduction in the number of BrdU-positive cells, and a small, but not significant reduction in the number of phH3 immunoreactive cells (Fig. 6A–H), which together speaks for a lowered proliferation rate after *fgf3* impairment. In parallel, we noticed an increased number of cleaved Caspase 3 (cCasp3) immunoreactive cells (Fig. 6I-K) showing elevated levels of cell

Biology Open (2019) 8, bio040683. doi:10.1242/bio.040683

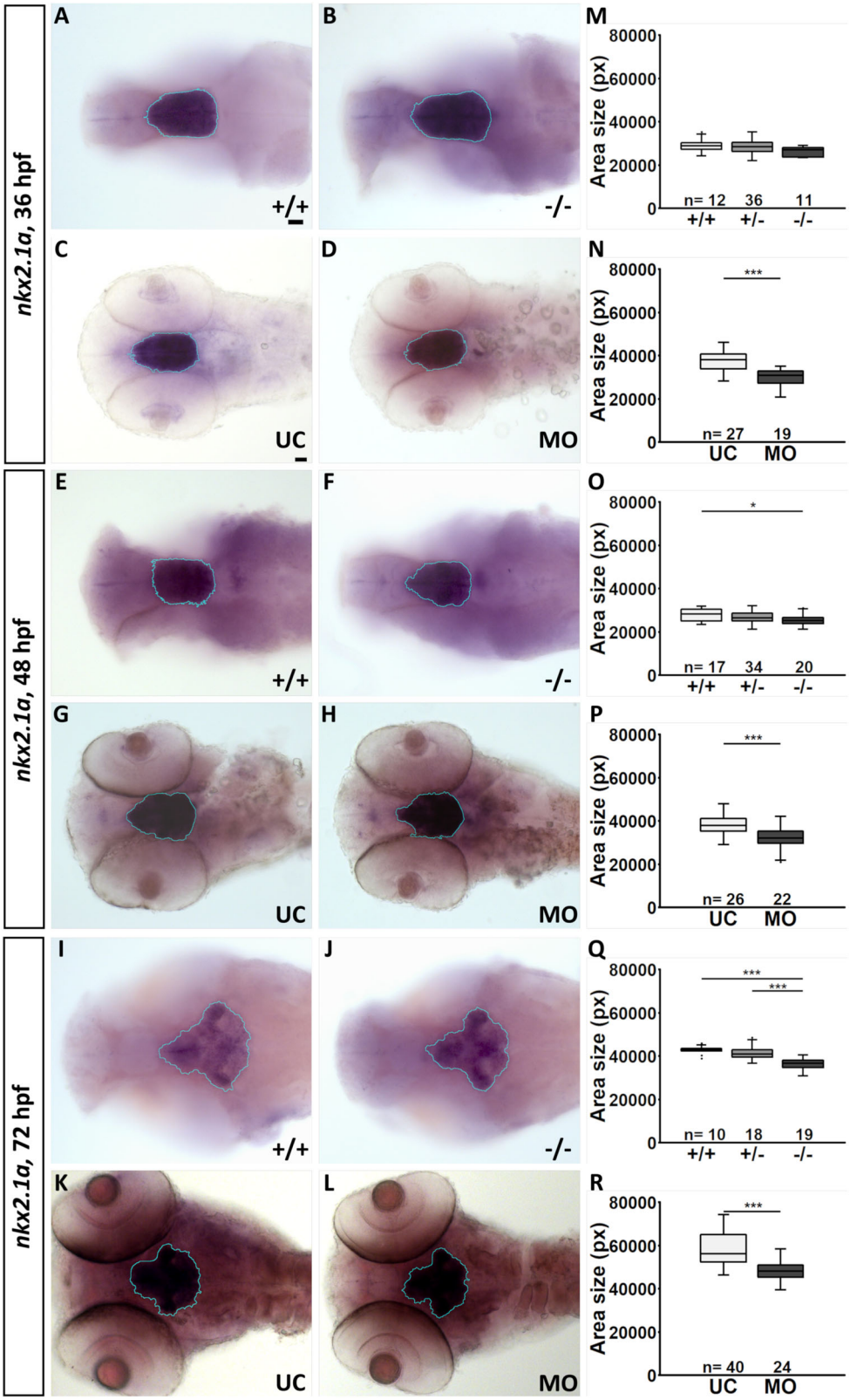


**Fig. 5. The size of the hypothalamic *nkx2.4b* domain is significantly reduced in *fgf3*$^{t24152}$ mutants and *fgf3* morphants.** (A–L) Light microscopic pictures showing expression of *nkx2.4b* in wild type (+/+) and homozygous *fgf3*$^{t24152}$ mutant (–/–) siblings as well as *fgf3* morphants (MO) and uninjected control siblings (UC) at 36, 48 and 72 hpf visualised by RNA *in situ* hybridisation. Outlines of semi-automated measurements of hypothalamic area are highlighted in blue. Ventral views, anterior to the left. Scale bars: 30 µm. (M–R) Area measurements (pixels) in *fgf3*$^{t24152}$ mutants, *fgf3* morphants and control siblings. Tukey boxplots show median, 25–75% percentile, IQR whiskers and outliers. *n*=number of analysed individuals +/–, heterozygous *fgf3*$^{t24152}$ mutants. **P*>0.05, ****P*>0.001.

death. Control experiments of *fgf3* morphants showed no significant alteration of the total body length (Fig. S6J), nor increased levels of cell death revealed by Acridine Orange and cCasp3 in morphants compared to control siblings (Fig. S4), showing that there is no general growth retardation or increased cell death due to loss of Fgf3 or morpholino injections.

### *fgf3*$^{t24152}$ mutant and morphant Fgf3 may still interact with Fgf receptors

To estimate the impact of the *fgf3*$^{t24152}$ mutation and the exon2/intron2 splice blocking morpholino on the folding, stability and receptor binding capacity of the truncated isoforms of Fgf3 we carried out computational 3D modelling comparing both truncated

Biology Open (2019) 8, bio040683. doi:10.1242/bio.040683

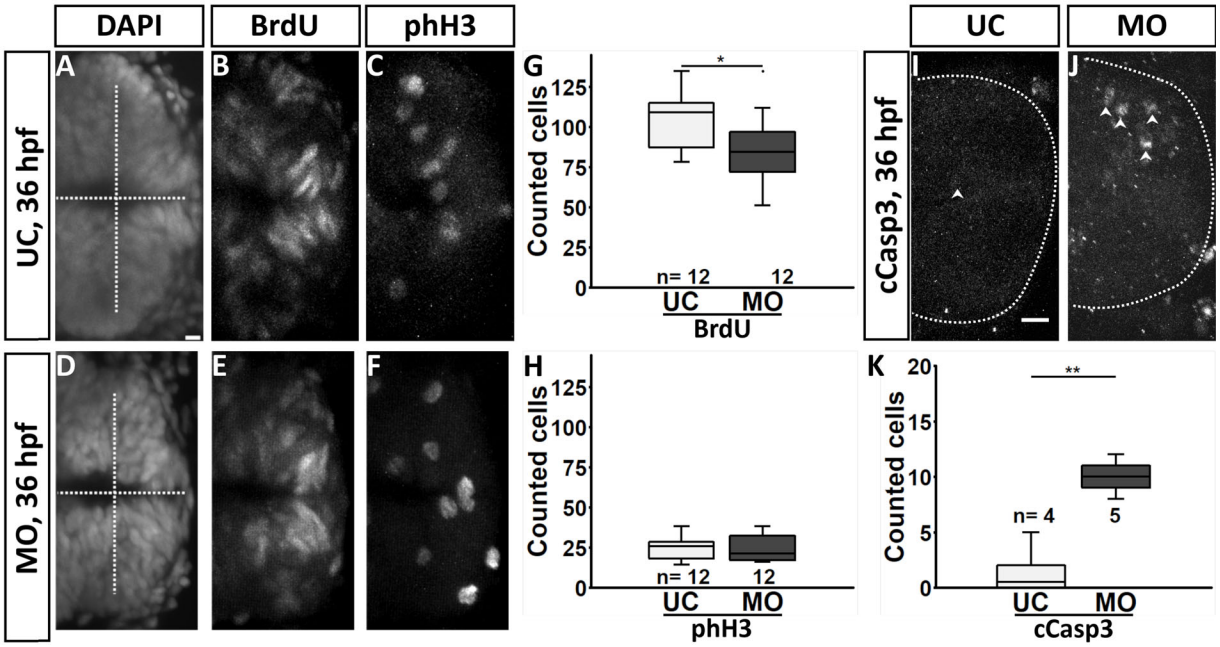


**Fig. 6. *fgf3* impairment results in reduced proliferation and increased cell death in the posterior hypothalamus at 36 hpf.** (A–F,I,J) Confocal maximum intensity projections of uninjected control (UC) and *fgf3* morphant (MO) siblings immunostained for BrdU and phospho-histone H3 (phH3) counterstained with DAPI, or for cleaved caspase 3 (cCasp3) at 36 hpf. Dashed lines indicate ventricle in A and D, and outer posterior border of the hypothalamus in I and J. Examples of cCasp3 positive cells are indicated (arrowheads). Anterior is to the left. Scale bars: 10 µm. (G,H,K) Quantifications of BrdU, phH3 and cCasp3 positive cells after *fgf3* impairment. Tukey boxplots show median, 25–75% percentile, IQR whiskers and outliers. *n*=number of analysed individuals. **P*>0.05, ***P*>0.01.

isoforms to wild-type Fgf3 (Fig. 7). As described above, the *fgf3*$^{t24152}$ mutation resulted in an Fgf3 isoform with about 70% of the wild-type amino acid sequence remaining, while the splice morpholino generated an isoform with about 50% of the wild-type sequence intact (Fig. S1D). Notably, receptor binding is likely to still be possible for the *fgf3*$^{t24152}$ mutant Fgf3 since a major portion of the interfaces with the Fgf receptor may remain intact (Fig. 7B). As expected the 3D model of the morpholino knockdown isoform of Fgf3 showed less preserved structure than the *fgf3*$^{t24152}$ isoform and therefore a lower probability to interact with the receptor (Fig. 7C). Both isoforms are likely to be less stable than wild-type Fgf3.

### *fgf3*$^{t24152}$ mutants exhibit minor alterations in the hypothalamic *fgf* transcriptome

The paracrine family of Fgf ligands includes multiple members in addition to Fgf3 (Itoh, 2007). Further, Fgf-signalling contains numerous regulatory feedback systems (Ornitz and Itoh, 2015). Therefore, it may be that one or several previously overseen Fgfs and/or that the feedback systems compensate for a loss of Fgf3 functionality. Such compensatory mechanisms could in turn explain why some of the posterior monoaminergic CSF-c and *avp*-expressing cells remain after *fgf3* impairment. To test this possibility, we accomplished a transcriptome analysis.

RNA sequencing was performed on dissected hypothalami of homozygous *fgf3*$^{t24152}$ mutants and wild-type cousins at 3 and 7 dpf (Fig. 8A). Our data analyses of 31 known zebrafish *fgf* genes (Table S4) revealed that transcripts for other previously overseen *fgfs* are present in wild types and mutants (Fig. 8B). In addition to *fgf3*, *fgf4* and *fgf8a* transcripts, which were already found in the developing hypothalamus (Herzog et al., 2004; Jackman et al., 2004; Liu et al., 2013; Reifers et al., 1998), we detected 13 further *fgf* transcripts in all groups: *fgf2*, *fgf6a*, *fgf8b*, *fgf11b*, *fgf12a*, *fgf12b*, *fgf13a*, *fgf13b*, *fgf14*, *fgf18a*, *fgf18b*, *fgf20a* and *fgf24*. Of these, *fgf3*, *fgf12a*, *fgf20a* and *fgf24* were differentially expressed at 3 and 7 dpf in the wild type (Fig. 7C). Interestingly, of the 16 detected *fgfs*, only *fgf3* was upregulated in mutants at both 3 and 7 dpf compared to wild types of the same age (Fig. 8C), which indicates a self-compensatory mechanism of *fgf3*. *fgf11b* and *fgf24* were up- and downregulated, respectively, in mutants compared to wild types, but only at 7 dpf (Fig. 8C). All other detected *fgfs* did not pass our 1.5-fold change criteria for the mutant versus wild type comparisons. Moreover, our RNA sequencing data showed that all five *fgfr* genes were expressed in the hypothalamus of all groups (Fig. 8B). In the wild-type groups, *fgfr2*, *fgfr3* and *fgfr4* were downregulated at 7 dpf compared to 3 dpf (Fig. 8C). Four out of four selected ETS-domain transcription factors, including *etv1*, *etv4*, *etv5a* and *etv5b*, were expressed in the hypothalamus of all groups (Fig. 8B). Of these ETS-domain factors only *etv5a* expression increased beyond our predefined fold change threshold from 3 to 7 dpf in wild types, but did not change when comparing mutants to wild types at 3 or 7 dpf (Fig. 8C). RNA sequencing results of Fgf-signalling pathway genes revealed that 56 out of 62 selected genes (Table S4) are expressed in the hypothalamus of wild types and mutants at 3 and 7 dpf (Fig. 8D). None of these 56 genes were differentially expressed when comparing mutants and wild types at 3 dpf, but at 7 dpf, *dusp1*, *dusp2* and *dusp5* were downregulated in the mutants (Fig. 7E).

Next, we tested two Fgf-signalling target genes, which exhibited distinct expression profiles in the RNA sequencing analysis, by RNA *in situ* hybridisation at 36 hpf after morpholino knockdown, namely *dusp1* and *dusp6*. In line with the RNA sequencing, *dusp1* showed low expression levels in the hypothalamus and a mild reduction after *fgf3* impairment in the hypothalamus as well as elsewhere in the central nervous system. *dusp6* expression was more prominent in the posterior hypothalamus, but did not reveal any obvious alterations in expression levels after *fgf3* impairment (Fig. S7). Thus, the *in situ* hybridisation analyses showed similar

Biology Open (2019) 8, bio040683. doi:10.1242/bio.040683

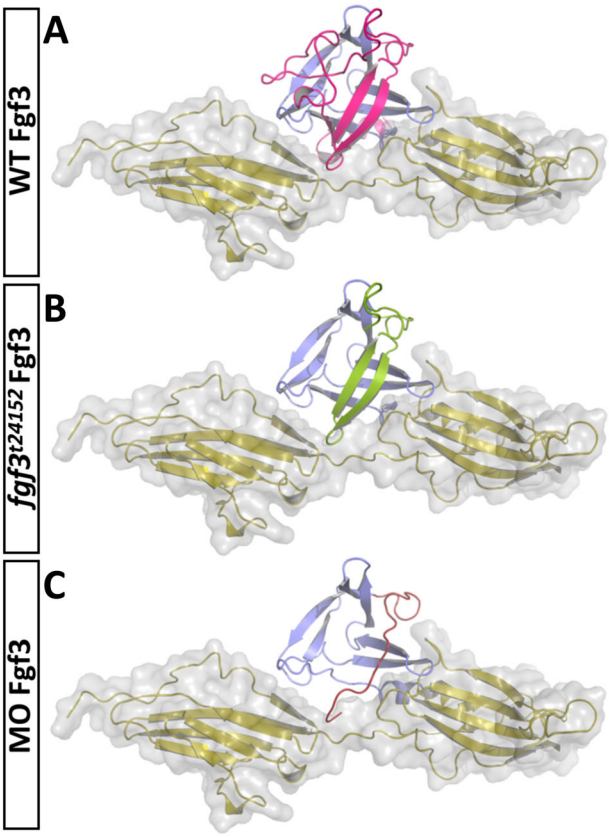


**Fig. 7. Ribbon representation of models of zebrafish Fgf3 isoforms bound to a FGF1 receptor.** (A) Ribbon representation of a zebrafish Fgf3 model (blue and pink) bound to a FGF1 receptor (yellow). The overall part affected by the *fgf3*$^{t24152}$ mutation or the *fgf3* morpholino is coloured in pink. (B) The deleted region of the *fgf3*$^{t24152}$ mutant isoform is omitted. The part that remains (green) as compared to the morpholino knockdown isoform still folds. Notably, receptor binding would be still possible if the variant maintains partial folding, since most of the interfaces with the FGF1 receptor would stay intact. (C) Model of the morpholino knockdown. The exchanged sequence is coloured in red. In comparison to the *fgf3*$^{t24152}$ mutant model it lacks even more structural elements rendering a correct folding and residual receptor interactions less likely.

results as the RNA sequencing data and indicate that Fgf-signalling is still present after *fgf3* impairment.

In summary, our RNA sequencing data showed that transcripts for previously overseen Fgf ligands are present in the developing wild-type hypothalamus. However, except for *fgf3* and *fgf11b*, neither of these were notably differentially regulated in the *fgf3*$^{t24152}$ mutant. Furthermore, the alterations in the downstream Fgf-signalling pathway were moderate. This suggests that only minor compensatory mechanisms are at hand in the *fgf3*$^{t24152}$ mutant and/or that the truncated Fgf3 isoform resulting from the *fgf3*$^{t24152}$ mutation is still, at least partly, functional.

## DISCUSSION

In this study we identify Fgf3 as the main Fgf ligand regulating the ontogeny of monoaminergic CSF-c and of *avp*-expressing cells in the zebrafish posterior hypothalamus. The requirement of Fgf3 follows a posterior to anterior gradient. Further, we show that Fgf3 controls expression of the ETS-domain transcription factor *etv5b*. Based on our current observations that *fgf3* expression precedes that of *tph1a* and 5-HT by several hours (Bellipanni et al., 2002; Bosco et al., 2013), and that the *nkx2.4b*-positive hypothalamic domain is smaller after *fgf3* impairment before the appearance of mature serotonergic CSF-c cells, we propose that Fgf3 is critical during early stages when progenitors are still proliferating. This is supported by our observation that the number of proliferating cells is decreased in parallel with increased cell death after *fgf3* impairment. This is in line with our earlier finding that Fgf-signalling, via *etv5b*, influences the proliferation of hypothalamic serotonergic CSF-c progenitor cells (Bosco et al., 2013). Furthermore, our present study provides evidence for the expression of previously overseen *fgfs* in the developing hypothalamus. We show that the expression of *fgf3* is upregulated upon impairment of *fgf3*, suggesting activation of a self-compensatory mechanism. Together these findings highlight Fgf-signalling, in particular Fgf3, in a novel context as part of a signalling pathway of critical importance for hypothalamic development. Our results have implications for the understanding of vertebrate hypothalamic evolution.

### *fgf3* is present in the posterior hypothalamus and likely acts as a morphogen regulating the expression of ETS-domain transcription factors

Fgf-signalling, acting via Etv5b, is an important pathway for development of serotonergic CSF-c cells in the posterior hypothalamus (Bosco et al., 2013) as well as in other contexts (Mason, 2007; Ornitz and Itoh, 2015; Raible and Brand, 2001; Roehl and Nüsslein-Volhard, 2001; Roussigné and Blader, 2006). However, the Fgf ligands are many and their interactions with Fgfrs are promiscuous (Ornitz and Itoh, 2015). To identify the Fgf ligand active in the developing posterior hypothalamus we searched existing expression data and found that *fgf3* is present in its most posterior region (Herzog et al., 2004), an area that contains serotonergic CSF-c cells (Lillesaar, 2011; McLean and Fetcho, 2004). Thus, we hypothesised that Fgf3 is the main ligand responsible for Fgf activity in this particular region of the brain. As observed elsewhere (Herzog et al., 2004; Liu et al., 2013), we confirmed that *fgf3* is expressed in the developing hypothalamus. Initially it has a broad distribution in the hypothalamic primordium. The expression then gradually becomes limited to the most posterior end in medially located cells surrounding the ventricle. Conforming to Fgf3 activity in the posterior hypothalamus, the Fgf responsive downstream targets *etv4*, *etv5a* and *etv5b* are present there, and largely overlap with *fgf3* at early stages (Fig. 1P,U) (Bosco et al., 2013). However, at later stages and in contrast to *fgf3* their expression is not limited to cells at the ventricle, but shows a broader distribution including cells in the parenchyme (Fig. 1Q,R,V) (Bosco et al., 2013), thus, fitting the role of Fgf3 as a morphogen (Bökel and Brand, 2013; Ornitz and Itoh, 2015). To test if Fgf3 regulates *etv5b* expression in the hypothalamus we analysed *etv5b* expression in *fgf3*$^{t24152}$ mutants and *fgf3* morphants. We noticed a reduction of *etv5b* transcripts in the posterior hypothalamus. These results demonstrate that Fgf3 is an important Fgf ligand in the developing posterior hypothalamus and that Fgf3 positively regulates *etv5b* expression in this brain region. Based on the distribution of transcripts it can be assumed that Fgf3 is secreted by a limited population of cells located at the ventricle, and reaches responsive cells expressing *etv5b* in more lateral positions. Based on our current findings we cannot conclude if *fgf3* alone regulates *etv5b* and if the regulation is direct or indirect.

### Fgf3 activity is critical for monoaminergic CSF-c and *avp*-expressing cells in the posterior hypothalamus

Hypothalamic serotonergic progenitors proliferate at around 36 hpf, and differentiated serotonergic CSF-c cells are detectable at 62 hpf

Biology Open (2019) 8, bio040683. doi:10.1242/bio.040683

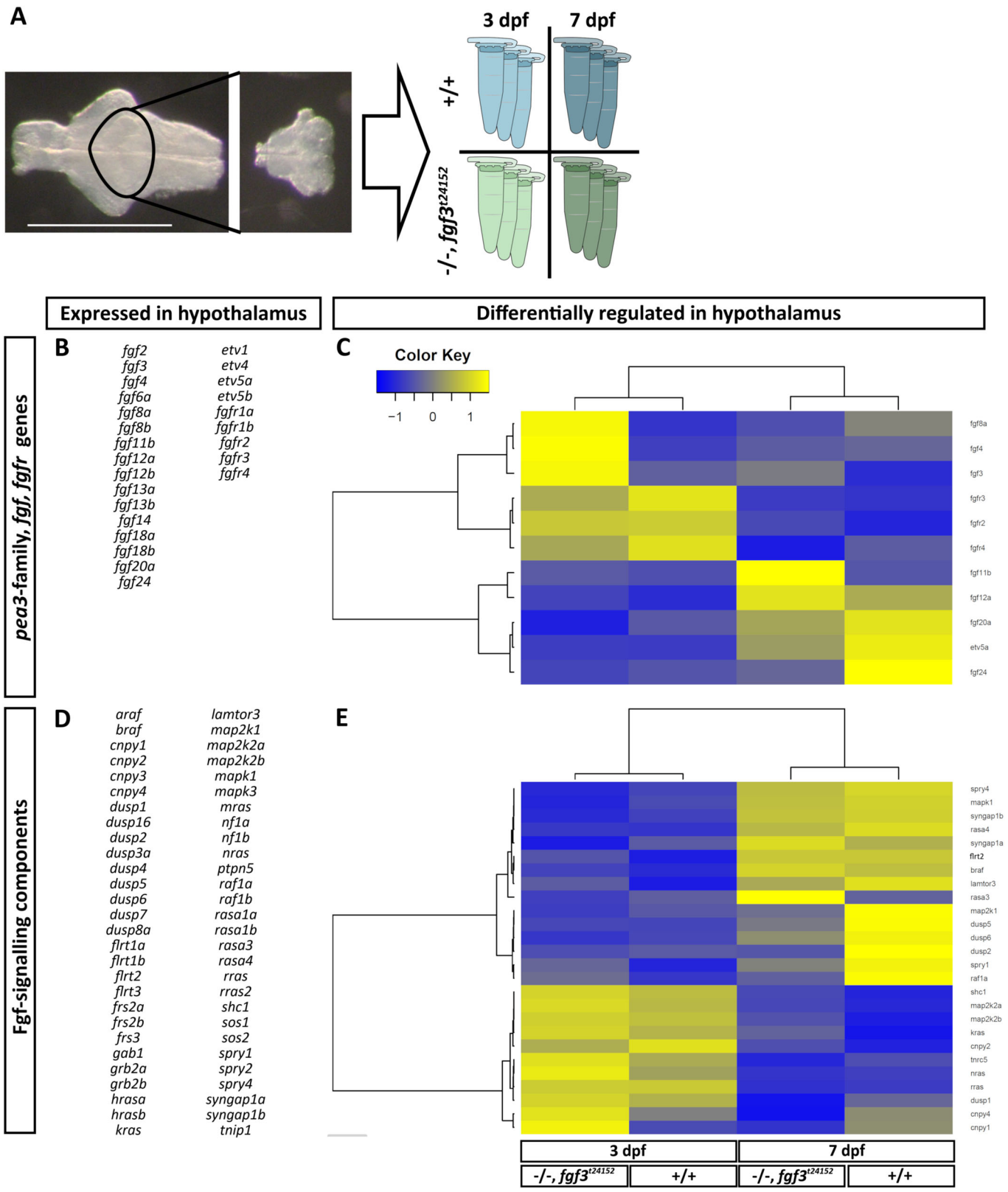


**Fig. 8.** See next page for legend.

in the i./p. cluster (Bosco et al., 2013; McLean and Fetcho, 2004). Further, *etv5b* regulates the proliferation of serotonergic progenitors, and ultimately the number of mature serotonergic CSF-c cells (Bosco et al., 2013). These observations, in combination with our current finding that Fgf3 impacts on *etv5b* expression, prompted us to investigate whether impairment of *fgf3* would reduce the number of serotonergic CSF-c cells. By impairing *fgf3* we show that, indeed, serotonergic CSF-c cells depend on Fgf3.

Biology Open (2019) 8, bio040683. doi:10.1242/bio.040683

**Fig. 8. Hierarchical clustering of hypothalamic Fgf-signalling pathway genes and downstream targets analysed in *fgf3*$^{t24152}$ mutants (−/−) and wild types (+/+) at 3 and 7 dpf.** (A) Scheme illustrating sample preparation and groups used for RNA sequencing. Micrographs show the dissected hypothalamic area (ventral view, anterior to the left) collected from wild types (blue tubes) and *fgf3*$^{t24152}$ mutants (green tubes) at 3 (light tubes) and 7 dpf (dark tubes). For each group, three independent tissue collections were performed resulting in a total of 12 samples processed for RNA sequencing. Scale bar: 500 µm. (B,D) List of *fgfs*, *fgfrs*, Fgf downstream target genes and Fgf-signalling components expressed (base mean ≥10) in the hypothalamus of −/− and +/+ embryos. All genes except *shc2* pass the base mean threshold in all four groups. *shc2* does not pass the base mean threshold in the 3 dpf −/− group. (C,E) Heat maps of differentially regulated (base mean ≥10, fold change ≥1.5) *fgfs, fgfrs* and Fgf downstream target genes (C) as well as Fgf-signalling components (E) in the hypothalamus of −/− and +/+ embryos. Columns represent z-score of mean values of replicates for each analysed group and rows depict individual genes. Colour key displays z-score ranging from ≥−1.5 to ≤1.5. Colour intensity represents expression levels of a gene for each group with blue or yellow indicating low or high expression.

Irrespective of the approach used, we always observed a reduction of hypothalamic serotonergic CSF-c cells. However, the population was never completely abolished, suggesting that some cells are independent of Fgf3, that our loss-of-function approaches result in only partial *fgf3*/Fgf3 impairment and/or that other Fgfs can partly compensate for the loss of *fgf3*/Fgf3 (for further details see below).

In the hypothalamus, dopaminergic CSF-c cells located in regions DC 4/5/6 and DC 7 are situated next to or intermingled with 5-HT immunoreactive cells of the i. and p. populations, respectively (Kaslin and Panula, 2001; McLean and Fetcho, 2004; Rink and Wullimann, 2002). Dopaminergic and serotonergic cells belong to the monoaminergic systems and accordingly share the expression of metabolic pathway genes, such as *ddc*, *mao* and *slc18a2* (*vmat2*) (Yamamoto and Vernier, 2011). This may suggest a common developmental programme for hypothalamic monoaminergic populations, and therefore a mutual dependence on Fgf3. To test if the dopaminergic DC 4/5/6 and DC 7 cells require Fgf3, we quantified them after *fgf3* impairment. Interestingly, we noticed a significant reduction only in the posteriorly located DC 7 population. Similarly, another study showed fewer dopaminergic cells specifically in the DC 7 population of *fgf3*$^{t24152}$ mutants (Koch et al., 2014). In contrast, neither the DC 4/5/6 nor the DC 7 populations are affected in *etv5b* morphants (Bosco et al., 2013). To further expand the analysis of hypothalamic cell populations potentially affected by Fgf3 we investigated neuroendocrine cells expressing *oxt*, *avp* and *cort* (Devos et al., 2002; Eaton et al., 2008; Unger and Glasgow, 2003). Of these neuroendocrine populations, the *oxt*- and *cort*-expressing ones were unaffected in *fgf3*$^{t24152}$ and *fgf3* morphants. Earlier quantifications of *oxt*- and *cort*-expressing cells in *etv5b* morphants (Bosco et al., 2013) are similar to our present results after *fgf3* impairment. Hence, we conclude that those two neuroendocrine populations are neither dependent on Etv5b nor Fgf3. In contrast, the number of *avp*-expressing cells was reduced in mutants and morphants suggesting that *avp*-expressing cells require Fgf3. Notably, the posterior *avp*-expressing cells were more affected than the anterior ones, similar to our observations of the dopaminergic DC 7 and DC 4/5/6 cells, thus supporting the hypothesis that Fgf3 plays a role predominantly in the posterior hypothalamus. Further, the *avp*-expressing population appears to be *etv5b* independent (Bosco et al., 2013). To summarise, the monoaminergic as well as *avp*-expressing cell populations require Fgf3. However, when comparing the different populations they exhibit distinct Fgf-signalling profiles; (1) *etv5b* is essential only for the posterior serotonergic cells, and (2) there is a posterior to anterior Fgf3 dependence gradient with the highest requirement seen in the posterior populations. We cannot exclude that *etv5b*-independent cell types use another ETS-domain transcription factor activated by Fgf3. The presence of *etv5a* and *etv4* transcripts in this region (Bosco et al., 2013) renders such a scenario possible.

It has been proposed that species-specific developmental programmes may result in 'hypothalamic modules', which can be gained or lost during evolution (Xie and Dorsky, 2017). One striking example of such a putative module is the posterior paraventricular organ surrounding the posterior recess, which houses the monoaminergic CSF-c cells. This particular structure is found in teleosts, but absent in tetrapods (Xavier et al., 2017). Thus, it is plausible that Fgf3 and Etv5b are part of a developmental signalling programme promoting the formation of a posterior hypothalamic module.

### Fgf3 likely regulates proliferation of monoaminergic progenitors

The monoaminergic CSF-c cells constitute a considerably large population of cells in the posterior hypothalamus. We therefore hypothesised that loss of those cells, as seen after *fgf3* impairment, would be associated with a smaller hypothalamus. As expected we observed a reduction of the *nkx2.4b*-positive domain at 72 hpf, a stage when numerous monoaminergic cells are present. Interestingly, the size reduction was observable at stages before the appearance of mature monoaminergic cells. This suggests that Fgf3 activity plays a role prior to complete cell maturation, presumably at a stage when monoaminergic progenitors are still proliferating, which is in line with the proposed function of Etv5b (Bosco et al., 2013). Accordingly, we here showed that the number of proliferating cells is reduced in the posterior hypothalamus at 36 hpf after *fgf3* impairment. Further, we found that the number of cCasp3 immunoreactive cells was increased in the posterior hypothalamus. Notably, we did not observe any overall morphological signs of increased cell death or growth retardation in *fgf3*-impaired embryos (mutants, morphants or CRISPR/Cas9) at any stage investigated, and no general increase of cell death in *fgf3* morphants speaking against a generally increased cell death or developmental retardation. Taken together this demonstrates that *fgf3* is required for the regulation of proliferation of progenitors in the posterior hypothalamus. The increased levels of hypothalamic cell death may be explained by Fgf3 acting as a survival factor, and/or it may be a secondary consequence of progenitors failing to follow their normal cell cycle programme. With our current experiments we cannot rule out that Fgf3 may also impact on cell fate and differentiation. We conclude that the change in hypothalamic size as revealed by the size of the *nkx2.4b* positive domain is caused by two temporally distinct processes, first the early reduced proliferation and increased cell death, and second the failure to generate mature monoaminergic cells populating the posterior hypothalamus.

### The *fgf3*$^{t24152}$ mutant exhibits a milder phenotype than *fgf3* morphants or *fgf3* CRISPR/Cas9-injected embryos

All three strategies (mutant, morpholino and CRISPR/Cas9) to interrupt *fgf3* function resulted in a reduction of monoaminergic CSF-c cells, with up to about 50% loss of serotonergic CSF-c cells on average in *fgf3* CRISPR/Cas9-injected embryos. However, we never saw a complete loss of these cells. This may be explained by: (1) some wild-type Fgf3 remaining after manipulation, (2) that the *fgf3*$^{t24152}$ allele is not a amorph, hence, not leading to a complete loss

Biology Open (2019) 8, bio040683. doi:10.1242/bio.040683

of Fgf3 activity, (3) compensatory mechanisms (upregulation of *fgf3* itself, upregulation of other *fgfs*, alterations in the downstream Fgf-signalling pathway and/or in its feedback regulators) and/or (4) that some serotonergic cells develop independently of Fgf3.

Our 3D models of the proteins resulting from the *fgf3*$^{t24152}$ mutation and the morpholino knockdown suggest that both isoforms are less stable than the wild-type protein, with the morphant protein being the least stable. However, according to the 3D models showing the ligand/receptor complex, both truncated isoforms may still interact with Fgfrs (Fig. 7). Again, the morphant form exhibits the more severe alteration. In the morphant, wild-type transcripts are detectable, and it is therefore likely that we do not have a complete loss-of-function. The *fgf3*$^{t24152}$ allele was published as being a nonsense mutation likely to be amorphic leading to a truncated Fgf3 protein with a complete loss of activity (Herzog et al., 2004). Considering this, we expected the homozygous *fgf3*$^{t24152}$ mutant to exhibit a more severe hypothalamic phenotype than we observed. With the 3D models and our phenotypic characterisation of the *fgf3*$^{t24152}$ mutant at hand we question the previous conclusion that the *fgf3*$^{t24152}$ mutation is amorphic, and propose that the *fgf3*$^{t24152}$ allele rather corresponds to a hypomorphic mutation.

Our CRISPR/Cas9 experiments were performed in the F0 generation and the mutations will therefore consist of various indels and have a mosaic distribution. The target for our exon 1 guide RNA is situated 153 base pairs from the start codon. In the most severe indel mutation scenario we therefore expect to lose about 80% of the wild-type amino acid sequence. As can be expected in F0-injected embryos, we saw a more variable strength of the phenotype between individuals compared to *fgf3*$^{t24152}$ mutants or morphants. In some individuals we noticed an almost complete loss of the posterior monoaminergic cell populations, which correlated with a strongly reduced posterior hypothalamus (Fig. 3M–P). Although we cannot finally conclude from our current data, it is likely that such individuals have lost most, if not all, functional Fgf3. In future studies of stable *fgf3* CRISPR lines it will be interesting to see if there is a complete loss of the posterior hypothalamic CSF-c cells.

Our RNA sequencing results showed that several *fgf* genes are expressed in the hypothalamus making them possible candidates for compensatory mechanisms. Of these *fgf*s the only one being upregulated in homozygous *fgf3*$^{t24152}$ mutants and passing the defined fold change threshold both at 3 and 7 dpf was *fgf3* itself, arguing for a self-compensatory role. Further, *fgf11b* was upregulated in mutants, but only at 7 dpf. *fgf8a* also showed a mild upregulation, but did not pass the defined threshold. *fgf8a* transcripts have been detected by *in situ* hybridisation in the posterior hypothalamus, but are spatially more restricted compared to *fgf3* (Reifers et al., 1998). The differential expression of downstream Fgf-signalling and feedback regulator genes was moderate in the *fgf3*$^{t24152}$ mutants, but a few of them were downregulated at 7 dpf. Among these were three *dusp* genes (*dusp1*, *2* and *5*), which act as negative feedback regulators of mitogen-activated protein kinases (Caunt and Keyse, 2013; Ornitz and Itoh, 2015; Znosko et al., 2010). Also *dusp6* showed a mild downregulation, but did not fulfil our selection criteria. *In situ* hybridisation for *dusp1* and *dusp6* after *fgf3* impairment by morpholinos support these findings. Taken together, these results indicate that a loss of Fgf3 activity in the *fgf3*$^{t24152}$ mutant is compensated for, but only mildly, on multiple levels by both self-compensation and by other Fgf ligands, as well as by alterations in the downstream signalling.

In addition to Fgf-signalling, other signalling pathways and gene regulatory networks are active in the zebrafish developing posterior hypothalamus. For instance, *lef1*, a direct mediator of Wnt-signalling, is transcribed there, and is required for the expression of proneural and neuronal genes (Lee et al., 2006). A likely Wnt candidate in this context is Wnt8b (Lee et al., 2006). Supporting a role for Wnt-signalling in hypothalamic serotonergic neurogenesis, a subset of 5-HT immuno-reactive hypothalamic cells express Wnt-activity reporters (Lee et al., 2006; Wang et al., 2009, 2012). Further, functional studies have shown that hypothalamic Wnt-responsive cells are immature cells contributing to GABAergic and serotonergic populations (Wang et al., 2012). Impairment of *fezf2* in zebrafish results in fewer serotonergic, dopaminergic and oxytocinergic cells (Blechman et al., 2007; Guo et al., 1999; Jeong et al., 2006; Levkowitz et al., 2003; Rink and Guo, 2004), and at least for the dopaminergic populations this seems to involve a Fezf2-dependant regulation of the transcription factors Neurogenin 1 and Orthopedia (Jeong et al., 2006; Shimizu and Hibi, 2009; Blechman et al., 2007; Ryu et al., 2007). If, and to which extent, these signalling pathways interact with Fgf-signalling to promote the generation of monoaminergic CSF-c cells remains a subject of investigation.

## MATERIALS AND METHODS

### Fish husbandry and sample preparation

Two zebrafish (*Danio rerio*) strains were used for the experiments: AB/AB wild types and the *fgf3*$^{t24152}$ *N*-ethyl-*N*-nitrosourea mutant in a Tü/Tü background (*lia*) (Herzog et al., 2004). Animal husbandry followed the animal welfare regulations of the District Government of Lower Franconia, Germany. Embryos, staged according to Kimmel et al. (1995), were raised and maintained in Danieau's solution (Cold Spring Harb. Protoc., 2011) with a 14/10-h light/dark cycle at 28°C. To prevent pigmentation, 0.2 mM 1-phenyl-2-thiourea was added to Danieau's solution after 24 hpf. For immunohistochemistry or *in situ* hybridisation, embryos were dechorionated and fixed for 24 h at 4°C in 4% paraformaldehyde in phosphate buffered saline (PBS), subsequently dehydrated in increasing concentrations of methanol and stored in 100% methanol at −20°C.

### Genotyping

Embryos with the *fgf3*$^{t24152}$ allele were genotyped by PCR using HiDi SNP DNA Polymerase (Genaxxon Bioscience). The polymerase allowed for allele specific discrimination of the gene fragment containing the point mutation *fgf3*$^{t24152}$ (G to A transition). Two PCR reactions were prepared to genotype each embryo. For the first reaction a forward (fwd) primer in which the last nucleotide at the 3′ end (G) was specific to the wild-type allele (fwd primer wild type: 5′GCCAGTTCTAAAAGGCAGTG**G**3′), and for the second reaction a fwd primer in which the last nucleotide at the 3′ end (A) was specific to the mutant allele (fwd primer mutant: 5′GCCAGTTCTAAAAGGCAGTG**A**3′) were used, respectively. The reverse (rev) primer was identical for both reactions (rev primer: 5′TGCCGCTGACTCTCTCTAAG3′). Both PCR products were run on a 1.5% agarose gel. Depending on the embryo's genotype, either a single band for the wild-type primer reaction (genotype: +/+), or a single band for the mutant primer reaction (genotype: −/−) was detectable. For the heterozygote genotype (+/−) a band was present in both reactions.

### *fgf3* impairment using morpholino and CRISPR/Cas9

For a morpholino-based knockdown of *fgf3,* 0.5 mM of a splice-blocking morpholino (5′CCCGACGTGACATAAACACTTACTGA3′, Gene Tools) targeting the splice donor site of exon 2/intron 2 of *fgf3* was injected into AB/AB fertilised eggs at the one-cell stage (Fig. S1). Blocking the splicing of *fgf3* pre-mRNA lead to partial and complete inclusion of intron 2, which in both cases generated a nonsense amino acid sequence with a stop, thus resulting in a truncated Fgf3 protein. Efficiency of the splice morpholino was evaluated by reverse transcription (RT)-PCR using RevertAid First Strand cDNA Synthesis Kit (Thermo Fisher Scientific) and GoTaq polymerase (Promega) according to manufacturer's instructions. The PCR products were separated on a 1.5% agarose gel, the bands were gel extracted

Biology Open (2019) 8, bio040683. doi:10.1242/bio.040683

using the GenElute Gel Extraction Kit (Sigma-Aldrich) and verified by Sanger sequencing (Eurofins).

For the *fgf3* CRISPR/Cas9 strategy two different gRNAs targeting exon 1 and exon 2 of *fgf3* (Fig. S2) were designed using the web tool CHOPCHOP (Labun et al., 2016; Montague et al., 2014). gRNA oligos (Table S1) were annealed, cloned into vector DR274 (a kind gift from Keith Joung Addgene plasmid #42250), *in vitro* transcribed using T7 RNA polymerase (a kind gift from Thomas Ziegenhals and Utz Fisher) and purified by Roti-Aqua-phenol/chloroform/isoamylalcohol (Roth) extraction. AB/AB embryos were co-injected at the one-cell stage with a cocktail containing both gRNAs (100–125 ng/µl each) and Cas9-NLS protein (300 ng/µl, *S. pyogenes*, New England Biolabs). To verify that the gRNAs induced indel mutations at the expected sites of *fgf3*, the target sites were amplified by PCR using fwd and rev primers listed in Table S1 followed by separation of the PCR products on a 3% high-resolution NuSieve 3:1 agarose gel (Lonza), PCR clean up using the GenElute PCR Clean-up Kit (Sigma-Aldrich) and Sanger sequencing (Eurofins).

For both, morpholino and CRISPR/Cas9, strategies uninjected stage matched siblings were used as controls. Additionally, Cas9-NLS protein only injected embryos were used as injection controls for the CRISPR/Cas9 experiments.

### Morpholino toxicity assay using Acridine Orange

Live 24 hpf *fgf3* morpholino-injected embryos and uninjected wild-type controls were incubated in 5 µg/ml Acridine Orange dissolved in Danieau's solution for 30 min at 28°C, rinsed and imaged to reveal cell death.

### BrdU labelling

*fgf3* morpholino-injected and wild-type control siblings were pulsed with 10 mM 5-bromo-2′-deoxyuridine (BrdU, Sigma-Aldrich) in 15% DMSO in Danieau's solution at 36 hpf for 20 min on ice, rinsed and directly fixed.

### Immunohistochemistry

BrdU and phH3 whole-mount immunohistochemistry was performed on embryos at 36 hpf. After rehydration embryos were pre-treated with 10 µg/ml proteinase K for 20 min, followed by antigen retrieval in 2 N HCl for 1 h and neutralisation with 0.1 M borate buffer (pH 8.5) for 20 min. Prior to whole-mount immunohistochemistry for cleaved caspase 3 (cCasp3) 36 hpf embryos were permeabilised first in 100% acetone for 7 min at −20°C and then in 50% methanol in PBT for 1 h at −20°C followed by a quick rinse in $H_2O$. Before labelling with BrdU and phH3 or cCasp3 antibodies the embryos were incubated in BrdU immuno blocking buffer [10% normal sheep serum, 0.2% bovine serum albumin in PBS with 0.1% Tween 20 (PBT) and 1% DMSO] for 1 h at room temperature. 5-HT and TH1 immunohistochemistry was performed on embryos with heads dissected free of skin, eyes and jaws for better antibody penetration. Dissected embryos were incubated in immunoblocking buffer (10% normal sheep serum, 0.2% bovine serum albumin in PBT) for 2 h at room temperature. Embryos were subsequently labelled with rat anti-BrdU (1:200; BU1-75, antibodies-online), rabbit anti-phH3 (1:300; 06-570, Millipore), rabbit anti-cCasp3 (1:500; 9664, Cell Signalling), mouse anti-TH1 (1:500; MAB318, Millipore) and rabbit anti-5-HT (1:1000; S5545, Sigma-Aldrich) diluted in respective blocking buffers for 3 days at 4°C with gentle shaking. After washes in PBT, to reveal immunoreactivity, the specimens were incubated for 2 days at 4°C in secondary antibodies conjugated with either Alexa Fluor 488 (goat anti-rabbit, 1:1000; A-11034, Thermo Fisher Scientific) and/or Alexa Fluor 568 (donkey anti-mouse, 1:1000; A-10037, Thermo Fisher Scientific) diluted in respective blocking buffer.

### Whole-mount RNA *in situ* hybridisation

To detect mRNA transcripts whole-mount *in situ* hybridisation was performed on fixed embryos as described elsewhere (Thisse and Thisse, 2008). In brief, *in vitro* transcribed digoxygenin (DIG) or fluorescein (fluo) labelled antisense RNA probes (Table S2) were synthesised using linearised plasmid template DNA, suitable RNA polymerases and DIG or fluo RNA labelling mix (Roche) following manufacturer's recommendations. Prehybridisation, hybridisation and stringency washes were performed at 65°C. Alkaline phosphatase conjugated to anti-DIG (1:5000, Roche) or anti-fluo (1:2000, Roche) Fab fragments were used to label hybridised transcripts, and to enable subsequent colour precipitation with NBT/BCIP solution (Roche) or Fast Red tablets (Sigma-Aldrich) dissolved in 0.1 M Tris-HCl with 0.1% Tween 20. For double *in situ* hybridisation, embryos were first labelled with anti-fluo antibody, which was revealed using Fast Red followed by heat detachment at 68°C for 2 h in PBT, followed by anti-DIG antibody labelling and NBT/BCIP revealing.

### Cryosections

For histology, embryos were cryo sectioned after *in situ* hybridisation. Specimens were cryoprotected in 15% sucrose in PBS overnight, followed by embedding in 7.5% porcine skin gelatine (300 Bloom, Sigma-Aldrich):15% sucrose solution in PBS. Gelatine blocks were cut and snap frozen in 2-methylbutane cooled down in a liquid nitrogen and were then stored at −80°C. 20 µm thick frontal crossections were cut on a cryostat (Microm HM 500 OM), collected on SuperFrost Plus slides (Thermo Fisher Scientific), rinsed in PBS and coverslipped.

### Sample preparation and data analysis of RNA sequencing

Hypothalami of 3 and 7 dpf homozygous wild-type embryos (Tü/Tü) and *fgf3*$^{t24152}$ homozygous mutant embryos (in Tü/Tü background) were dissected (Fig. 8A). Wild-type embryos were generated by crossing previously identified homozygous wild-type adult fish, which were siblings to the heterozygous parents used to generate *fgf3*$^{t24152}$ homozygous mutant embryos. Thus, the homozygous wild type and the *fgf3*$^{t24152}$ homozygous mutant embryos used for the RNA sequencing analysis were cousins. The *fgf3*$^{t24152}$ homozygous mutant embryos were identified by their characteristic fused otolith phenotype (Herzog et al., 2004). Dissections were performed on ice in a petri dish containing ice cold slicing solution (234 mM sucrose, 11 mM D-glucose, 2.5 mM KCl, 1.25 mM $NaH_2PO_4$, 0.5 mM $CaCl_2$, 2.0 mM $MgSO_4$, 26 mM $NaHCO_3$) (Ma et al., 2015) using forceps. To collect sufficient material for RNA sequencing (∼100 ng total RNA) hypothalami were pooled. For each of the four groups (3 and 7 dpf wild-type and mutant embryos) three independent replicates were collected adding up to a total of 12 samples. The collected tissue was preserved in RNA*later* RNA stabilisation solution (Qiagen) until RNA was isolated using RNeasy Mini Kit (Qiagen) according to manufacturer's instructions. RNA Library preparation was performed by the Core Unit Systems Medicine of the University of Würzburg according to the Illumina TruSeq stranded mRNA Sample Preparation Guide with 100 ng of input RNA and 15 PCR cycles. All 12 libraries were pooled and sequenced on a NextSeq 500 with a read length of 150 nt. Sequenced reads were mapped with the RNA-Seq aligner software STAR (Dobin et al., 2013) to the Ensembl *Danio rerio* genome version GRCz10. Expected read counts were calculated by RSEM (Li and Dewey, 2011). For detection of differentially expressed genes the Bioconductor/R package DESeq2 was used (Love et al., 2014). From our RNA sequencing data, we decided to focus on a total of 82 genes relevant for Fgf-signalling, including *fgf* genes, *fgf* receptor genes, Fgf-signalling pathway genes and Fgf downstream target genes. Genes were chosen according to Itoh (2007), Ornitz and Itoh (2015), zfin.org and the KEGG pathway mapping tool (Kanehisa and Goto, 2000). Heat maps with dendrograms were generated using R (package 'made4'). Genes with a base mean of ≥10 in all four groups were considered as expressed in the hypothalamus. Genes with a base mean ≥10 and a fold change ≥1.5 were considered as differentially expressed. When a gene passed the selection criteria in at least one of the three comparisons (wild type at 3 versus 7 dpf, wild type versus mutant at 3 and 7 dpf) it was represented in the heat map.

### 3D structural analysis

For 3D modelling of the zebrafish Fgf3 structure the amino acid sequence was sent to the Phyre2 server (Kelley et al., 2015). 155 residues from the entire sequence were modelled with a 100% confidence level using pdb entry 1ihk (Plotnikov et al., 2001) and were subsequently used for the structural assessment of the Fgf3 variants. The structure of Fgf3 wild-type protein as well as truncated Fgf3 mutant (*fgf3*$^{t24152}$) and morphant protein were modelled bound to a human FGF1 receptor based on the pdb entry 3ojv (Beenken et al., 2012). The structures were visualised with PyMOL

(PyMOL Molecular Graphics System, version 2.0, Schrödinger, LLC) and superpositions were performed in coot (Emsley et al., 2010).

### Image acquisition, cell quantification and measurements

Prior to image acquisition live embryos were mounted in 3% methylcellulose in Danieau's solution. Embryos processed for whole-mount *in situ* hybridisation, cryosectioning and immunohistochemistry were mounted in 80% glycerol in PBT. Images were acquired using a stereo microscope (M205FA, Leica) with Leica Application Suit 3.8.0 (Leica) software for live images, a light microscope (Axiophot, Zeiss) with AxioVision Rel. 4.8 software (Zeiss) for whole-mount *in situ* hybridisations or confocal microscopes (Eclipse Ti, Nikon or DMIRE2 SP2 system, Leica) with NIS Elements AR 3.22.15 (Nikon) or TCS (Leica) software for fluorescent stainings.

For cell quantifications and measurements Fiji 1.8.0 imaging software (Schindelin et al., 2012) with the BioVoxxel Image Processing and Analysis Toolbox (Brocher, 2015) was used. Further, area measurements of the hypothalamic region stained for *nkx2.4b* were obtained through semi-automatic image analysis followed by manual validation and, if required, manual correction of the computed area. Fish body length was manually measured as a straight line from the most anterior to the most posterior end of the fish. All quantifications were done double blinded. Z-stacks of confocal images were collapsed into maximum intensity projections for the figure panels. Background subtraction, as well as brightness and contrast adjustments were performed on the entire image during figure preparation using Fiji 1.8.0 imaging software (Schindelin et al., 2012) with the BioVoxxel Image Processing and Analysis Toolbox (Brocher, 2015) and GIMP 2.10 (The GIMP Team).

### Statistical analysis

Rstudio 1.0.143 (Rstudio, Inc.) was used for statistical analysis and graph design. Median and median absolute deviation (MAD) were calculated for each group and are presented in Table S3. Normal distribution was calculated using the Shapiro-Wilk test. If the null hypothesis for normal distribution was accepted a parametric test was used, either a two-sample *t*-test or a one-way ANOVA depending on number of groups. If the null hypothesis for normal distribution was rejected a non-parametric test was used, either a Mann–Whitney-*U*-test or a Kruskal–Wallis test depending on number of groups. For multiple group comparisons Tukey's Honest Significance Differences or Nemenyi tests were used as post hoc tests following a one-way ANOVA or a Kruskal–Wallis test, respectively. Results were considered significant with a *P*-value of 0.05 or lower. Significance levels of 0.05, 0.01 and 0.001 are indicated in the graphs with one, two or three asterisks, respectively.

#### Acknowledgements

We are grateful to M. Schartl for generously providing access to fish facility and lab infrastructure. Furthermore, we are thankful to C. Drepper, S. Meierjohann and C. Stigloher for discussions and input on the project. The *fgf3*$^{t24152}$ mutant was kindly provided by the M. Hammerschmidt lab, and plasmids for *in situ* hybridisation probes by L. Bally-Cuif and K. Yamamoto.

#### Competing interests

The authors declare no competing or financial interests.

#### Author contributions

Conceptualization: I.R., K.-P.L., C.L.; Methodology: I.R., S.K., J.K., C.L.; Software: S.K., J.K.; Validation: I.R., J.J., S.K., J.K., C.L.; Formal analysis: I.R., S.K., J.K., C.L.; Investigation: I.R., J.J., C.L.; Resources: C.L.; Data curation: I.R., J.J., S.K., J.K., C.L.; Writing - original draft: I.R., C.L.; Writing - review & editing: I.R., J.J., S.K., J.K., K.-P.L., C.L.; Visualization: I.R., J.J., S.K., J.K., C.L.; Supervision: K.-P.L., C.L.; Project administration: K.-P.L., C.L.; Funding acquisition: K.-P.L., C.L.

#### Funding

The Zonta Club Würzburg, Interdisziplinäres Zentrum für Klinische Forschung (IZKF No. N-320) Würzburg and the Faculty of Biology, University of Würzburg supported this work (C.L.). I.R. was funded by a grant of the German Excellence Initiative to the Graduate School of Life Sciences (GSLS), University of Würzburg. C.L. was funded by the Bayerische Gleichstellungsförderung (BGF). This publication was funded by the German Research Foundation (DFG) and the University of Würzburg in the funding programme Open Access Publishing. K.-P.L. and, in part I.R., are supported by the German Research Foundation (DFG: CRC TRR 58 A1/A5, No. 44541416), the Horizon 2020 Research and Innovation Programme (Eat2beNICE, No. 728018), ERA-Net NEURON/DECODE! (No. FKZ01EW1902), and 5-100 Russian Academic Excellence Project.

#### Data availability

RNA-seq data have been deposited at the National Center for Biotechnology Information (NCBI) with accession number PRJNA541414.

#### Supplementary information

Supplementary information available online at http://bio.biologists.org/lookup/doi/10.1242/bio.040683.supplemental

#### References

**Anichtchik, O., Sallinen, V., Peitsaro, N. and Panula, P.** (2006). Distinct structure and activity of monoamine oxidase in the brain of zebrafish (Danio rerio). *J. Comp. Neurol.* **498**, 593-610. doi:10.1002/cne.21057

**Ballion, B., Branchereau, P., Chapron, J. and Viala, D.** (2002). Ontogeny of descending serotonergic innervation and evidence for intraspinal 5-HT neurons in the mouse spinal cord. *Dev. Brain Res.* **137**, 81-88. doi:10.1016/S0165-3806(02)00414-5

**Beenken, A., Eliseenkova, A. V., Ibrahimi, O. A., Olsen, S. K. and Mohammadi, M.** (2012). Plasticity in interactions of fibroblast growth factor 1 (FGF1) N terminus with FGF receptors underlies promiscuity of FGF1. *J. Biol. Chem.* **287**, 3067-3078. doi:10.1074/jbc.M111.275891

**Bellipanni, G., Rink, E. and Bally-Cuif, L.** (2002). Cloning of two tryptophan hydroxylase genes expressed in the diencephalon of the developing zebrafish brain. *Mech. Dev.* **119**, Suppl. 1, S215-S220. doi:10.1016/s0925-4773(03)00119-9

**Biran, J., Tahor, M., Wircer, E. and Levkowitz, G.** (2015). Role of developmental factors in hypothalamic function. *Front. Neuroanat.* **9**, 47. doi:10.3389/fnana.2015.00047

**Blechman, J., Borodovsky, N., Eisenberg, M., Nabel-Rosen, H., Grimm, J. and Levkowitz, G.** (2007). Specification of hypothalamic neurons by dual regulation of the homeodomain protein Orthopedia. *Development* **134**, 4417-4426. doi:10.1242/dev.011262

**Bökel, C. and Brand, M.** (2013). Generation and interpretation of FGF morphogen gradients in vertebrates. *Curr. Opin. Genet. Dev.* **23**, 415-422. doi:10.1016/j.gde.2013.03.002

**Bosco, A., Bureau, C., Affaticati, P., Gaspar, P., Bally-Cuif, L. and Lillesaar, C.** (2013). Development of hypothalamic serotoninergic neurons requires Fgf signalling via the ETS-domain transcription factor Etv5b. *Development* **140**, 372-384. doi:10.1242/dev.089094

**Brocher, J.** (2015). *The BioVoxxel Image Processing and Analysis Toolbox*. Paris, France: EuBIAS-Conference.

**Burbridge, S., Stewart, I. and Placzek, M.** (2016). Development of the neuroendocrine hypothalamus. *Comprehensive Physiology* **13**, 623-643. doi:10.1002/cphy.c150023

**Caunt, C. J. and Keyse, S. M.** (2013). Dual-specificity MAP kinase phosphatases (MKPs). *FEBS J.* **280**, 489-504. doi:10.1111/j.1742-4658.2012.08716.x

**Chen, Y.-C., Priyadarshini, M. and Panula, P.** (2009). Complementary developmental expression of the two tyrosine hydroxylase transcripts in zebrafish. *Histochem. Cell Biol.* **132**, 375-381. doi:10.1007/s00418-009-0619-8

**Cold Spring Harb. Protoc.** (2011). Danieau's solution (30×) pdb.rec12467. doi:10.1101/pdb.rec12467

**Curran, K. P. and Chalasani, S. H.** (2012). Serotonin circuits and anxiety: what can invertebrates teach us? *Invert. Neurosci.* **12**, 81-92. doi:10.1007/s10158-012-0140-y

**Deneris, E. and Gaspar, P.** (2018). Serotonin neuron development: shaping molecular and structural identities. *WIREs Dev. Biol.* **7**, e301. doi:10.1002/wdev.301

**Deneris, E. S. and Wyler, S. C.** (2012). Serotonergic transcriptional networks and potential importance to mental health. *Nat. Neurosci.* **15**, 519-527. doi:10.1038/nn.3039

**Devos, N., Deflorian, G., Biemar, F., Bortolussi, M., Martial, J. A., Peers, B. and Argenton, F.** (2002). Differential expression of two somatostatin genes during zebrafish embryonic development. *Mech. Dev.* **115**, 133-137. doi:10.1016/S0925-4773(02)00082-5

**Dobin, A., Davis, C. A., Schlesinger, F., Drenkow, J., Zaleski, C., Jha, S., Batut, P., Chaisson, M. and Gingeras, T. R.** (2013). STAR: ultrafast universal RNA-seq aligner. *Bioinformatics* **29**, 15-21. doi:10.1093/bioinformatics/bts635

**Duncan, R. N., Xie, Y., McPherson, A. D., Taibi, A. V., Bonkowsky, J. L., Douglass, A. D. and Dorsky, R. I.** (2016). Hypothalamic radial glia function as self-renewing neural progenitors in the absence of Wnt/β-catenin signaling. *Development* **143**, 45-53. doi:10.1242/dev.126813

**Eaton, J. L., Holmqvist, B. and Glasgow, E.** (2008). Ontogeny of vasotocin-expressing cells in zebrafish: Selective requirement for the transcriptional regulators orthopedia and single-minded 1 in the preoptic area. *Dev. Dyn.* **237**, 995-1005. doi:10.1002/dvdy.21503

**Ekström, P., Nyberg, L. and van Veen, T.** (1985). Ontogenetic development of serotoninergic neurons in the brain of a teleost, the three-spined stickleback. An immunohistochemical analysis. *Brain Res.* **349**, 209-224. doi:10.1016/0165-3806(85)90145-2

**Emsley, P., Lohkamp, B., Scott, W. G. and Cowtan, K.** (2010). Features and development of Coot. *Acta Cryst. D* **66**, 486-501. doi:10.1107/S0907444910007493

**Filippi, A., Mahler, J., Schweitzer, J. and Driever, W.** (2009). Expression of the paralogous tyrosine hydroxylase encoding genes th1 and th2 reveals the full complement of dopaminergic and noradrenergic neurons in zebrafish larval and juvenile brain. *J. Comp. Neurol.* **518**, 423-438. doi:10.1002/cne.22213

**Flames, N. and Hobert, O.** (2011). Transcriptional control of the terminal fate of monoaminergic neurons. *Annu. Rev. Neurosci.* **34**, 153-184. doi:10.1146/annurev-neuro-061010-113824

**Fossat, P., Bacqué-Cazenave, J., Deurwaerdère, P. D., Delbecque, J.-P. and Cattaert, D.** (2014). Anxiety-like behavior in crayfish is controlled by serotonin. *Science* **344**, 1293-1297. doi:10.1126/science.1248811

**Gillette, R.** (2006). Evolution and function in serotonergic systems. *Integr. Comp. Biol.* **46**, 838-846. doi:10.1093/icb/icl024

**Guo, S., Wilson, S. W., Cooke, S., Chitnis, A. B., Driever, W. and Rosenthal, A.** (1999). Mutations in the Zebrafish unmask shared regulatory pathways controlling the development of catecholaminergic neurons. *Dev. Biol.* **208**, 473-487. doi:10.1006/dbio.1999.9204

**Hammond, K. L. and Whitfield, T. T.** (2011). Fgf and Hh signalling act on a symmetrical pre-pattern to specify anterior and posterior identity in the zebrafish otic placode and vesicle. *Development* **138**, 3977-3987. doi:10.1242/dev.066639

**Hay-Schmidt, A.** (2000). The evolution of the serotonergic nervous system. *Proc. R. Soc. B Biol. Sci.* **267**, 1071-1079. doi:10.1098/rspb.2000.1111

**Herzog, W., Sonntag, C., Hardt, S. von der, Roehl, H. H., Varga, Z. M. and Hammerschmidt, M.** (2004). Fgf3 signaling from the ventral diencephalon is required for early specification and subsequent survival of the zebrafish adenohypophysis. *Development* **131**, 3681-3692. doi:10.1242/dev.01235

**Itoh, N.** (2007). The Fgf families in humans, mice, and Zebrafish: their evolutional processes and roles in development, metabolism, and disease. *Biol. Pharm. Bull.* **30**, 1819-1825. doi:10.1248/bpb.30.1819

**Jackman, W. R., Draper, B. W. and Stock, D. W.** (2004). Fgf signaling is required for zebrafish tooth development. *Dev. Biol.* **274**, 139-157. doi:10.1016/j.ydbio.2004.07.003

**Jeong, J.-Y., Einhorn, Z., Mercurio, S., Lee, S., Lau, B., Mione, M., Wilson, S. W. and Guo, S.** (2006). Neurogenin1 is a determinant of zebrafish basal forebrain dopaminergic neurons and is regulated by the conserved zinc finger protein Tof/Fezl. *Proc. Natl. Acad. Sci. USA* **103**, 5143-5148. doi:10.1073/pnas.0600337103

**Kanehisa, M. and Goto, S.** (2000). KEGG: kyoto encyclopedia of genes and genomes. *Nucleic Acids Res.* **28**, 27-30. doi:10.1093/nar/28.1.27

**Kapsimali, M., Caneparo, L., Houart, C. and Wilson, S. W.** (2004). Inhibition of Wnt/Axin/β-catenin pathway activity promotes ventral CNS midline tissue to adopt hypothalamic rather than floorplate identity. *Development* **131**, 5923-5933. doi:10.1242/dev.01453

**Kaslin, J. and Panula, P.** (2001). Comparative anatomy of the histaminergic and other aminergic systems in zebrafish (Danio rerio). *J. Comp. Neurol.* **440**, 342-377. doi:10.1002/cne.1390

**Kass-Simon, G. and Pierobon, P.** (2007). Cnidarian chemical neurotransmission, an updated overview. *Comp. Biochem. Physiol. A. Mol. Integr. Physiol.* **146**, 9-25. doi:10.1016/j.cbpa.2006.09.008

**Kelley, L. A., Mezulis, S., Yates, C. M., Wass, M. N. and Sternberg, M. J.** (2015). The Phyre2 web portal for protein modelling, prediction and analysis. *Nat. Protoc.* **10**, 845-858. doi:10.1038/nprot.2015.053

**Kimmel, C. B., Ballard, W. W., Kimmel, S. R., Ullmann, B. and Schilling, T. F.** (1995). Stages of embryonic development of the zebrafish. *Dev. Dyn.* **203**, 253-310. doi:10.1002/aja.1002030302

**Kiyasova, V. and Gaspar, P.** (2011). Development of raphe serotonin neurons from specification to guidance. *Eur. J. Neurosci.* **34**, 1553-1562. doi:10.1111/j.1460-9568.2011.07910.x

**Koch, P., Löhr, H. B. and Driever, W.** (2014). A mutation in cnot8, component of the Ccr4-not complex regulating transcript stability, affects expression levels of developmental regulators and reveals a role of Fgf3 in development of caudal hypothalamic dopaminergic neurons. *PLoS ONE* **9**, e113829. doi:10.1371/journal.pone.0113829

**Labun, K., Montague, T. G., Gagnon, J. A., Thyme, S. B. and Valen, E.** (2016). CHOPCHOP v2: a web tool for the next generation of CRISPR genome engineering. *Nucleic Acids Res.* **44**, W272-W276. doi:10.1093/nar/gkw398

**Lee, J. E., Wu, S.-F., Goering, L. M. and Dorsky, R. I.** (2006). Canonical Wnt signaling through Lef1 is required for hypothalamic neurogenesis. *Development* **133**, 4451-4461. doi:10.1242/dev.02613

**Levkowitz, G., Zeller, J., Sirotkin, H. I., French, D., Schilbach, S., Hashimoto, H., Hibi, M., Talbot, W. S. and Rosenthal, A.** (2003). Zinc finger protein *too few* controls the development of monoaminergic neurons. *Nat. Neurosci.* **6**, 28-33. doi:10.1038/nn979

**Li, B. and Dewey, C. N.** (2011). RSEM: accurate transcript quantification from RNA-Seq data with or without a reference genome. *BMC Bioinformatics* **12**, 323. doi:10.1186/1471-2105-12-323

**Lillesaar, C.** (2011). The serotonergic system in fish. *J. Chem. Neuroanat.* **41**, 294-308. doi:10.1016/j.jchemneu.2011.05.009

**Lillesaar, C., Tannhäuser, B., Stigloher, C., Kremmer, E. and Bally-Cuif, L.** (2007). The serotonergic phenotype is acquired by converging genetic mechanisms within the zebrafish central nervous system. *Dev. Dyn.* **236**, 1072-1084. doi:10.1002/dvdy.21095

**Lillesaar, C., Stigloher, C., Tannhäuser, B., Wullimann, M. F. and Bally-Cuif, L.** (2009). Axonal projections originating from raphe serotonergic neurons in the developing and adult zebrafish, Danio rerio, using transgenics to visualize raphe-specific pet1 expression. *J. Comp. Neurol.* **512**, 158-182. doi:10.1002/cne.21887

**Liu, F., Pogoda, H.-M., Pearson, C. A., Ohyama, K., Löhr, H., Hammerschmidt, M. and Placzek, M.** (2013). Direct and indirect roles of Fgf3 and Fgf10 in innervation and vascularisation of the vertebrate hypothalamic neurohypophysis. *Development* **140**, 1111-1122. doi:10.1242/dev.080226

**Love, M. I., Huber, W. and Anders, S.** (2014). Moderated estimation of fold change and dispersion for RNA-seq data with DESeq2. *Genome Biol.* **15**, 550. doi:10.1186/s13059-014-0550-8

**Lucki, I.** (1998). The spectrum of behaviors influenced by serotonin. *Biol. Psychiatry* **44**, 151-162. doi:10.1016/S0006-3223(98)00139-5

**Ma, Y., Juntti, S. A., Hu, C. K., Huguenard, J. R. and Fernald, R. D.** (2015). Electrical synapses connect a network of gonadotropin releasing hormone neurons in a cichlid fish. *Proc. Natl. Acad. Sci. USA* **112**, 3805-3810. doi:10.1073/pnas.1421851112

**Mason, I.** (2007). Initiation to end point: the multiple roles of fibroblast growth factors in neural development. *Nat. Rev. Neurosci.* **8**, 583-596. doi:10.1038/nrn2189

**Mathieu, J., Barth, A., Rosa, F. M., Wilson, S. W. and Peyriéras, N.** (2002). Distinct and cooperative roles for Nodal and Hedgehog signals during hypothalamic development. *Development* **129**, 3055-3065.

**McLean, D. L. and Fetcho, J. R.** (2004). Ontogeny and innervation patterns of dopaminergic, noradrenergic, and serotonergic neurons in larval zebrafish. *J. Comp. Neurol.* **480**, 38-56. doi:10.1002/cne.20280

**Montague, T. G., Cruz, J. M., Gagnon, J. A., Church, G. M. and Valen, E.** (2014). CHOPCHOP: a CRISPR/Cas9 and TALEN web tool for genome editing. *Nucleic Acids Res.* **42**, W401-W407. doi:10.1093/nar/gku410

**Montgomery, J. E., Wiggin, T. D., Rivera-Perez, L. M., Lillesaar, C. and Masino, M. A.** (2016). Intraspinal serotonergic neurons consist of two, temporally distinct populations in developing zebrafish. *Dev. Neurobiol.* **76**, 673-687. doi:10.1002/dneu.22352

**Moroz, L. L. and Kohn, A. B.** (2016). Independent origins of neurons and synapses: insights from ctenophores. *Philos. Trans. R. Soc. B Biol. Sci.* **371**, 20150041. doi:10.1098/rstb.2015.0041

**Muthu, V., Eachus, H., Ellis, P., Brown, S. and Placzek, M.** (2016). Rx3 and Shh direct anisotropic growth and specification in the zebrafish tuberal/anterior hypothalamus. *Development* **143**, 2651-2663. doi:10.1242/dev.138305

**Norton, W. H., Mangoli, M., Lele, Z., Pogoda, H.-M., Diamond, B., Mercurio, S., Russell, C., Teraoka, H., Stickney, H. L., Rauch, G.-J. et al.** (2005). Monorail/Foxa2 regulates floorplate differentiation and specification of oligodendrocytes, serotonergic raphé neurones and cranial motoneurones. *Development* **132**, 645-658. doi:10.1242/dev.01611

**Norton, W. H. J., Folchert, A. and Bally-Cuif, L.** (2008). Comparative analysis of serotonin receptor (HTR1A/HTR1B families) and transporter (slc6a4a/b) gene expression in the zebrafish brain. *J. Comp. Neurol.* **511**, 521-542. doi:10.1002/cne.21831

**Ornitz, D. M. and Itoh, N.** (2015). The fibroblast growth factor signaling pathway. *WIREs. Dev. Biol.* **4**, 215-266. doi:10.1002/wdev.176

**Plotnikov, A. N., Eliseenkova, A. V., Ibrahimi, O. A., Shriver, Z., Sasisekharan, R., Lemmon, M. A. and Mohammadi, M.** (2001). Crystal structure of fibroblast growth factor 9 reveals regions implicated in dimerization and autoinhibition. *J. Biol. Chem.* **276**, 4322-4329. doi:10.1074/jbc.M006502200

**Raible, F. and Brand, M.** (2001). Tight transcriptional control of the ETS domain factors Erm and Pea3 by Fgf signaling during early zebrafish development. *Mech. Dev.* **107**, 105-117. doi:10.1016/S0925-4773(01)00456-7

**Reifers, F., Bohli, H., Walsh, E. C., Crossley, P. H., Stainier, D. Y. and Brand, M.** (1998). Fgf8 is mutated in zebrafish acerebellar (ace) mutants and is required for maintenance of midbrain-hindbrain boundary development and somitogenesis. *Development* **125**, 2381-2395.

**Rink, E. and Guo, S.** (2004). The too few mutant selectively affects subgroups of monoaminergic neurons in the zebrafish forebrain. *Neuroscience* **127**, 147-154. doi:10.1016/j.neuroscience.2004.05.004

**Rink, E. and Wullimann, M. F.** (2002). Development of the catecholaminergic system in the early zebrafish brain: an immunohistochemical study. *Dev. Brain Res.* **137**, 89-100. doi:10.1016/S0165-3806(02)00354-1

**Roehl, H. and Nüsslein-Volhard, C.** (2001). Zebrafish pea3 and erm are general targets of FGF8 signaling. *Curr. Biol.* **11**, 503-507. doi:10.1016/S0960-9822(01)00143-9

**Roussigné, M. and Blader, P.** (2006). Divergence in regulation of the PEA3 family of ETS transcription factors. *Gene Expr. Patterns* **6**, 777-782. doi:10.1016/j.modgep.2006.01.008

**Ryu, S., Mahler, J., Acampora, D., Holzschuh, J., Erhardt, S., Omodei, D., Simeone, A. and Driever, W.** (2007). Orthopedia homeodomain protein is essential for diencephalic dopaminergic neuron development. *Curr. Biol.* **17**, 873-880. doi:10.1016/j.cub.2007.04.003

**Sallinen, V., Sundvik, M., Reenilä, I., Peitsaro, N., Khrustalyov, D., Anichtchik, O., Toleikyte, G., Kaslin, J. and Panula, P.** (2009). Hyperserotonergic phenotype after monoamine oxidase inhibition in larval zebrafish. *J. Neurochem.* **109**, 403-415. doi:10.1111/j.1471-4159.2009.05986.x

**Sano, Y., Ueda, S., Yamada, H., Takeuchi, Y., Goto, M. and Kawata, M.** (1983). Immunohistochemical demonstration of serotonin-containing CSF-contacting neurons in the submammalian paraventricular organ. *Histochemistry* **77**, 423-430. doi:10.1007/BF00495798

**Schindelin, J., Arganda-Carreras, I., Frise, E., Kaynig, V., Longair, M., Pietzsch, T., Preibisch, S., Rueden, C., Saalfeld, S., Schmid, B. et al.** (2012). Fiji: an open-source platform for biological-image analysis. *Nat. Methods* **9**, 676-682. doi:10.1038/nmeth.2019

**Shimizu, T. and Hibi, M.** (2009). Formation and patterning of the forebrain and olfactory system by zinc-finger genes Fezf1 and Fezf2. *Dev. Growth Differ.* **51**, 221-231. doi:10.1111/j.1440-169X.2009.01088.x

**Stach, T.** (2005). Comparison of the serotonergic nervous system among tunicata: implications for its evolution within chordata. *Org Div Evol* **5**, 15-24. doi:10.1016/j.ode.2004.05.004

**Teraoka, H., Russell, C., Regan, J., Chandrasekhar, A., Concha, M. L., Yokoyama, R., Higashi, K., Take-Uchi, M., Dong, W., Hiraga, T. et al.** (2004). Hedgehog and Fgf signaling pathways regulate the development of tphR-expressing serotonergic raphe neurons in zebrafish embryos. *J. Neurobiol.* **60**, 275-288. doi:10.1002/neu.20023

**Thisse, C. and Thisse, B.** (2008). High-resolution in situ hybridization to whole-mount zebrafish embryos. *Nat. Protoc.* **3**, 59-69. doi:10.1038/nprot.2007.514

**Topp, S., Stigloher, C., Komisarczuk, A. Z., Adolf, B., Becker, T. S. and Bally-Cuif, L.** (2008). Fgf signaling in the zebrafish adult brain: Association of Fgf activity with ventricular zones but not cell proliferation. *J. Comp. Neurol.* **510**, 422-439. doi:10.1002/cne.21802

**Trowbridge, S., Narboux-Nême, N. and Gaspar, P.** (2011). Genetic models of serotonin (5-HT) depletion: what do they tell us about the developmental role of 5-HT? *Anat. Rec.* **294**, 1615-1623. doi:10.1002/ar.21248

**Ugrumov, M. V., Taxi, J., Steinbusch, H. W., Tramu, G. and Mitskevich, M. S.** (1989). On the distribution and morpho-functional characteristics of 5-HT-immunoreactive cells in the hypothalamus of fetuses and neonatal rats. *Brain Res. Dev. Brain Res.* **46**, 233-241. doi:10.1016/0165-3806(89)90287-3

**Unger, J. L. and Glasgow, E.** (2003). Expression of isotocin-neurophysin mRNA in developing zebrafish. *Gene Expr. Patterns* **3**, 105-108. doi:10.1016/S1567-133X(02)00064-9

**Vígh, B., Manzano e Silva, M. J., Frank, C. L., Vincze, C., Czirok, S. J., Szabó, A., Lukáts, A. and Szél, A.** (2004). The system of cerebrospinal fluid-contacting neurons. Its supposed role in the nonsynaptic signal transmission of the brain. *Histol. Histopathol.* **19**, 607-628.

**Wang, X., Lee, J. E. and Dorsky, R. I.** (2009). Identification of Wnt-Responsive Cells in the Zebrafish Hypothalamus. *Zebrafish* **6**, 49-58. doi:10.1089/zeb.2008.0570

**Wang, X., Kopinke, D., Lin, J., McPherson, A. D., Duncan, R. N., Otsuna, H., Moro, E., Hoshijima, K., Grunwald, D. J., Argenton, F. et al.** (2012). Wnt Signaling Regulates Postembryonic Hypothalamic Progenitor Differentiation. *Dev. Cell* **23**, 624-636. doi:10.1016/j.devcel.2012.07.012

**Ware, M., Hamdi-Rozé, H. and Dupé, V.** (2014). Notch signaling and proneural genes work together to control the neural building blocks for the initial scaffold in the hypothalamus. *Front. Neuroanat.* **8**, 140. doi:10.3389/fnana.2014.00140

**Xavier, A. L., Fontaine, R., Bloch, S., Affaticati, P., Jenett, A., Demarque, M., Vernier, P. and Yamamoto, K.** (2017). Comparative analysis of monoaminergic cerebrospinal fluid-contacting cells in Osteichthyes (bony vertebrates). *J. Comp. Neurol.* **525**, 2265-2283. doi:10.1002/cne.24204

**Xie, Y. and Dorsky, R. I.** (2017). Development of the hypothalamus: conservation, modification and innovation. *Development* **144**, 1588-1599. doi:10.1242/dev.139055

**Yamamoto, K. and Vernier, P.** (2011). The evolution of dopamine systems in chordates. *Front. Neuroanat.* **5**, 21. doi:10.3389/fnana.2011.00021

**Yamamoto, K., Ruuskanen, J. O., Wullimann, M. F. and Vernier, P.** (2010). Two tyrosine hydroxylase genes in vertebrates: new dopaminergic territories revealed in the zebrafish brain. *Mol. Cell. Neurosci.* **43**, 394-402. doi:10.1016/j.mcn.2010.01.006

**Yamamoto, K., Ruuskanen, J. O., Wullimann, M. F. and Vernier, P.** (2011). Differential expression of dopaminergic cell markers in the adult zebrafish forebrain. *J. Comp. Neurol.* **519**, 576-598. doi:10.1002/cne.22535

**Znosko, W. A., Yu, S., Thomas, K., Molina, G. A., Li, C., Tsang, W., Dawid, I. B., Moon, A. M. and Tsang, M.** (2010). Overlapping functions of Pea3 ETS transcription factors in FGF signaling during zebrafish development. *Dev. Biol.* **342**, 11-25. doi:10.1016/j.ydbio.2010.03.011

# Supplementary data

**Table S1. Target sites, oligos and PCR primers for *fgf3* CRISPR/Cas9 approach.**

| | ***fgf3* exon 1 (5'-3')** | ***fgf3* exon 2 (5'-3')** |
|---|---|---|
| **Target site** | GGGGTTTACGAGCACCTCGG | GGCAATCAAGGGACTGTTTT |
| **Oligo 1** | TAGGGGTTTACGAGCACCTCGG | TAGGCAATCAAGGGACTGTTTT |
| **Oligo 2** | AAACCCGAGGTGCTCGTAAACC | AAACAAAACAGTCCCTTGATTG |
| **Primer fwd** | AGCTTCTTGGATCCGAGTTTGG | ATACGCTTTCAGACAAGGCAAT |
| **Primer rev** | GATCCGTCTATTTTCCCGTTCG | CCCGACGTGACATAACACTTAC |

**Table S2. RNA probes used for whole mount RNA *in situ* hybridisation.**

| Gene name | Gene symbol | Reference |
|---|---|---|
| *arginine vasopressin* | *avp* | Eaton et al., 2008 |
| *cortistatin* | *cort* | Devos et al., 2002 |
| *dual specificity phosphatase 1* | *dusp1* | this study |
| *dual specificity phosphatase 6* | *dusp6* | Tsang et al., 2004 |
| *ets variant 5b* | *etv5b* | Münchberg et al., 1999 |
| *fibroblast growth factor 3* | *fgf3* | Kiefer et al., 1996 |
| *NK2 homeobox 4b* | *nkx2.4b* | Rohr and Concha, 2000 |
| *oxytocin* | *oxt* | Unger and Glasgow, 2003 |
| *tyrosine hydroxylase 2* | *th2* | Yamamoto et al., 2010 |

**Table S3. Overview of counting of monoaminergic and neuroendocrine cells, and of measurements of the *nkx2.4b* expressing hypothalamic area in embryos after *fgf3* impairment.**

| | marker | 5–HT | | TH1 | | | | *th2* | *oxt* | *avp* | *cort* | *nkx2.4b* | | | | | | Fish length | phH3 | BrdU | cCasp3 |
|---|---|---|---|---|---|---|---|---|---|---|---|---|---|---|---|---|---|---|---|---|---|
| | region | i./p. | | DC 4/5/6 | | DC 7 | | DC 7 | | | | ventral | | | lateral | | | | | | |
| | hpf | 72 | 96 | 72 | 96 | 72 | 96 | 96 | 72 | 72 | 72 | 36 | 48 | 72 | 36 | 48 | 72 | 72 | 36 | 36 | 36 |
| *fgf3* morpholino | UC | 64 ±11 | 98 ±13 | 59 ±4 | 67 ±6 | 20 ±5 | 47 ±9 | 40 ±4 | 27.5 ±5 | 57 ±4 | 127.5 ±9.5 | 37950 ±3352 | 37920 ±3250 | 56190 ±4836 | 53270 ±3068 | 38100 ±6846 | 39410 ±5779 | 2464000 ±45710 | 25.5 ±7 | 109 ±16.5 | 0.5 ±0.5 |
| | n | 13 | 15 | 13 | 15 | 13 | 17 | 9 | 28 | 28 | 31 | 27 | 26 | 40 | 27 | 23 | 24 | 21 | 12 | | 5 |
| | MO | 35 ±6 | 66 ±7 | 52 ±2 | 62 ±6 | 6 ±4 | 31 ±3 | 27 ±7 | 27.5 ±7 | 51 ±6 | 128 ±14 | 30840 ±3067 | 32010 ±3085 | 48070 ±3066 | 42600 ±4084 | 30730 ±4183 | 37850 ±3597 | 2463000 ±78618 | 21 ±4.5 | 84.5 ±13.5 | 10±1 |
| | n | 19 | 17 | 19 | 17 | 19 | 17 | 11 | 24 | 20 | 25 | 19 | 22 | 24 | 18 | 24 | 24 | 13 | 12 | | 4 |
| | p | 4.56 $e^{-06}$ | 1.97 $e^{-06}$ | 0.191 | 0.1903 | 1.24 $e^{-05}$ | 9.53 $e^{-06}$ | 0.0011 | n.s. (0.3651) | 0.0003 | n.s. (0.5653) | 1.08 $e^{-06}$ | 0.0001 | 6.83 $e^{-09}$ | 4.383 $e^{-06}$ | n.s. (0.2) | n.s. (0.3137) | n.s. (0.8097) | n.s. (0.862) | 0.0408 | 0.0016 |
| *fgf3*$^{tl24152}$ mutant | +/+ | 60 ±22 | - | 58 ±6 | - | 11 ±4 | - | - | 27 ±4 | 61 ±7 | 86 ±10.5 | 28780 ±1832 | 28110 ±2861 | 42600 ±811 | - | - | - | - | - | - | - |
| | n | 23 | - | 25 | - | 25 | - | - | 14 | 18 | 20 | 12 | 17 | 10 | - | - | - | - | - | - | - |
| | +/- | 59.5 ±14 | - | 55 ±7 | - | 12 ±4 | - | - | 26 ±3 | 59.5 ±5 | 90 ±11 | 28310 ±2240 | 26390 ±1932 | 40870 ±1624 | - | - | - | - | - | - | - |
| | n | 46 | - | 51 | - | 51 | - | - | 38 | 26 | 41 | 36 | 34 | 18 | - | - | - | - | - | - | - |
| | -/- | 50 ±14.5 | - | 52.5 ±8.5 | - | 7.5 ±4.5 | - | - | 31 ±3 | 51 ±4 | 97 ±9 | 26950 ±1370 | 25160 ±1306 | 36670 ±1842 | - | - | - | - | - | - | - |
| | n | 18 | - | 20 | - | 20 | - | - | 19 | 15 | 16 | 11 | 20 | 19 | - | - | - | - | - | - | - |
| | p | 0.04 | - | n.s. (0.35) | - | 0.0097 | - | - | 0.0169 | 0.0024 | n.s. (0.492) | 0.0757 | 0.038 | 3.7 $e^{-08}$ | - | - | - | - | - | - | - |
| CRISPR/Cas9 | UC | 75 ±12 | - | 64.5 ±3 | - | 28.5 ±4.5 | - | - | - | - | - | - | - | - | - | - | - | - | - | - | - |
| | n | 12 | - | 12 | - | 12 | - | - | - | - | - | - | - | - | - | - | - | - | - | - | - |
| | C9C | 65.5 ±6 | - | 70.5 ±5.5 | - | 33 ±3.5 | - | - | - | - | - | - | - | - | - | - | - | - | - | - | - |
| | n | 16 | - | 16 | - | 16 | - | - | - | - | - | - | - | - | - | - | - | - | - | - | - |
| | CR | 38 ±16 | - | 62.5 ±5.5 | - | 18.5 ±6 | - | - | - | - | - | - | - | - | - | - | - | - | - | - | - |
| | n | 22 | - | 12 | - | 12 | - | - | - | - | - | - | - | - | - | - | - | - | - | - | - |
| | p | 0.0007 | - | n.s. (0.0917) | - | 1.31 $e^{-07}$ | - | - | - | - | - | - | - | - | - | - | - | - | - | - | - |

Cell numbers and area sizes (pixels) displayed as median±MAD. p = p-values determined by two-sample t-test, Mann-Whitney-U test, one-way ANOVA, or Kruskal-Wallis test. n = number of analysed individuals. UC, uninjected control; MO, morphant; C9C, Cas9 only injected control; CR, CRISPR/Cas9 injected

**Table S4: List of Fgf-signalling genes selected for expression analysis in the hypothalamus by RNA sequencing.**

***pea3*-family*, fgf, fgfr* genes:**

| | | | |
|---|---|---|---|
| *etv1* | *fgf6a* | *fgf12a* | *fgf20b* |
| *etv4* | *fgf6b* | *fgf12b* | *fgf21* |
| *etv5a* | *fgf7* | *fgf13a* | *fgf22* |
| *etv5b* | *fgf8a* | *fgf13b* | *fgf23* |
| *fgf1a* | *fgf8b* | *fgf14* | *fgf24* |
| *fgf1b* | *fgf9* | *fgf16* | *fgfr1a* |
| *fgf2* | *fgf10a* | *fgf18a* | *fgfr1b* |
| *fgf3* | *fgf10b* | *fgf18b* | *fgfr2* |
| *fgf4* | *fgf11a* | *fgf19* | *fgfr3* |
| *fgf5* | *fgf11b* | *fgf20a* | *fgfr4* |

**Fgf-signalling component genes:**

| | | | | | | |
|---|---|---|---|---|---|---|
| *araf* | *dusp3a* | *flrt3* | *kras* | *nf1b* | *rras2* | *tnip1* |
| *braf* | *dusp3b* | *frs2a* | *lamtor3* | *nras* | *shc1* | *tnip2* |
| *cnpy1* | *dusp4* | *frs2b* | *map2k1* | *ptpn5* | *shc2* | |
| *cnpy2* | *dusp5* | *frs3* | *map2k2a* | *raf1a* | *sos1* | |
| *cnpy3* | *dusp6* | *gab1* | *map2k2b* | *raf1b* | *sos2* | |
| *cnpy4* | *dusp7* | *grb2a* | *mapk1* | *rasa1a* | *spry1* | |
| *dusp1* | *dusp8a* | *grb2b* | *mapk3* | *rasa1b* | *spry2* | |
| *dusp10* | *flrt1a* | *hrasa* | *MRAS* | *rasa3* | *spry4* | |
| *dusp16* | *flrt1b* | *hrasb* | *mras* | *rasa4* | *syngap1a* | |
| *dusp2* | *flrt2* | *kl* | *nf1a* | *rras* | *syngap1b* | |

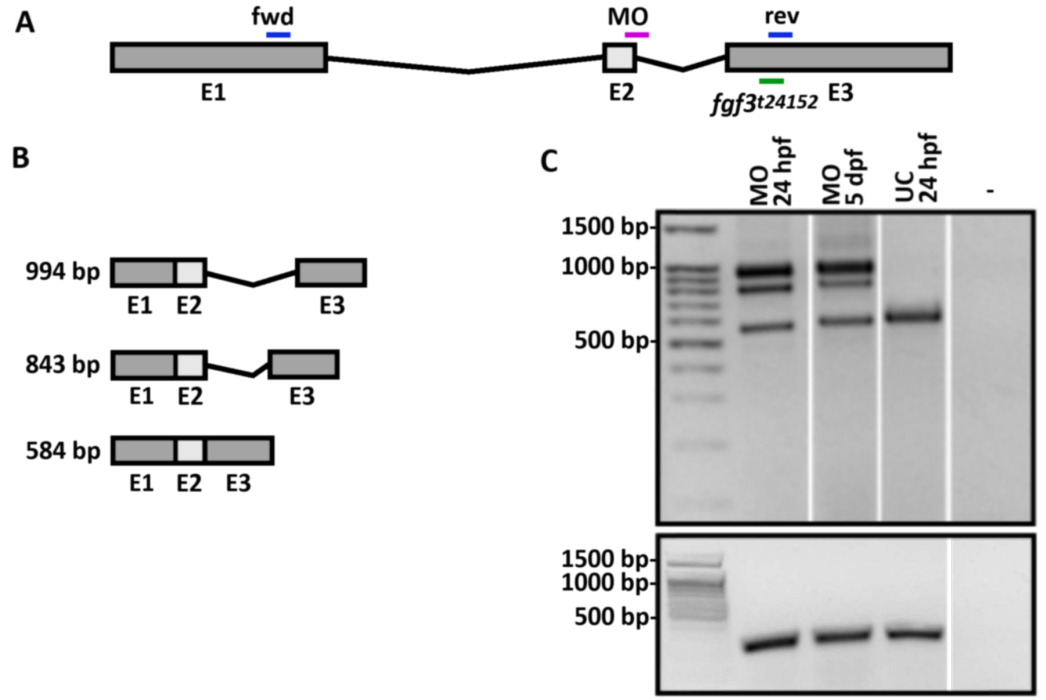


D

```
Fgf3 WT        1 MVIILLLLLLLSFLDPSLEESLAPRLTRTPRAPCARGQACDPRQRRDAGGR  50
Fgf3t24152     1 MVIILLLLLLLSFLDPSLEESLAPRLTRTPRAPCARGQACDPRQRRDAGGR  50
Fgf3 MO        1 MVIILLLLLLLSFLDPSLEESLAPRLTRTPRAPCARGQACDPRQRRDAGGR  50
                 **************************************************
Fgf3 WT       51 GGVYEHLGGAPRRRKLYCATKYHLQIHPNGKIDGSLEENNPLSILEITAV 100
Fgf3t24152    51 GGVYEHLGGAPRRRKLYCATKYHLQIHPNGKIDGSLEENNPLSILEITAV 100
Fgf3 MO       51 GGVYEHLGGAPRRRKLYCATKYHLQIHPNGKIDGSLEENNPLSILEITAV 100
                 **************************************************
Fgf3 WT      101 DVGVVAIKGLFSGRYLAMNEKGRLYASE-VF-NRECEFLERIHELGYNTY 148
Fgf3t24152   101 DVGVVAIKGLFSGRYLAMNEKGRLYASE-VF-NRECEFLERIHELGYNTY 148
Fgf3 MO      101 DVGVVAIKGLFSGRYLAMNEKGRLYASVSVMSRRENQVAEILLAVGSDND 150
                 **************************  *: .** :. * :  :* :.
Fgf3 WT      149 ASRHHATTQPPPTGSGIGGSKRRASSKRQWYVSINGKGRPRRGFKTRSTD 198
Fgf3t24152   149 ASRHHATTQPPPTGSGIGGSKRRASSKRQ*--------------------- 178
Fgf3 MO      151 *-------------------------------------------------

Fgf3 WT      199 KASLFLPRVLANKDHEMVRKLRESQRHHTGSHRAPVGRAERRRRRHRGSK 248
Fgf3t24152       --------------------------------------------------
Fgf3 MO          --------------------------------------------------

Fgf3 WT      249 GHNRRADI                                          256
Fgf3t24152       --------
Fgf3 MO          --------
```

**Fig. S1. *fgf3* morpholino (MO) knock-down efficiency and amino acid sequence alignment of wildtype (WT), mutant (*fgf3*$^{t24152}$) and morphant Fgf3. (A)** Scheme of *fgf3* gene and locations of splice MO target site (magenta), as well as forward (fwd) and reverse (rev) primers (blue) used for detection of morphant splice forms, and point mutation *fgf3*$^{t24152}$ (green). **(B)** Schematic representation of splice products detected by RT-PCR after MO injections. **(C)** RT-PCR results of morphants at 24 hpf and 5 dpf, uninjected control (UC) siblings at 24 hpf and water control (-) for *fgf3* (upper gel) and *β-actin* (lower gel). Additional RT-PCR products in *fgf3* morphants at 843 and 994 bp corresponded to a partial intron 2 inclusion due to a cryptic splice site or a complete inclusion of intron 2, respectively. **(D)** Amino acid sequence alignment of WT, *fgf3*$^{t24152}$ mutant and morphant Fgf3. The *fgf3*$^{t24152}$ mutation results in a premature stop after amino acid 177 (Q), thus, 69% of the WT protein sequence remains intact. After MO application, both splice forms of *fgf3* generate a nonsense sequence after amino acid 127 (S, magenta) and a stop after amino acid 150 (D), thus, 50% of the WT protein sequence is intact.

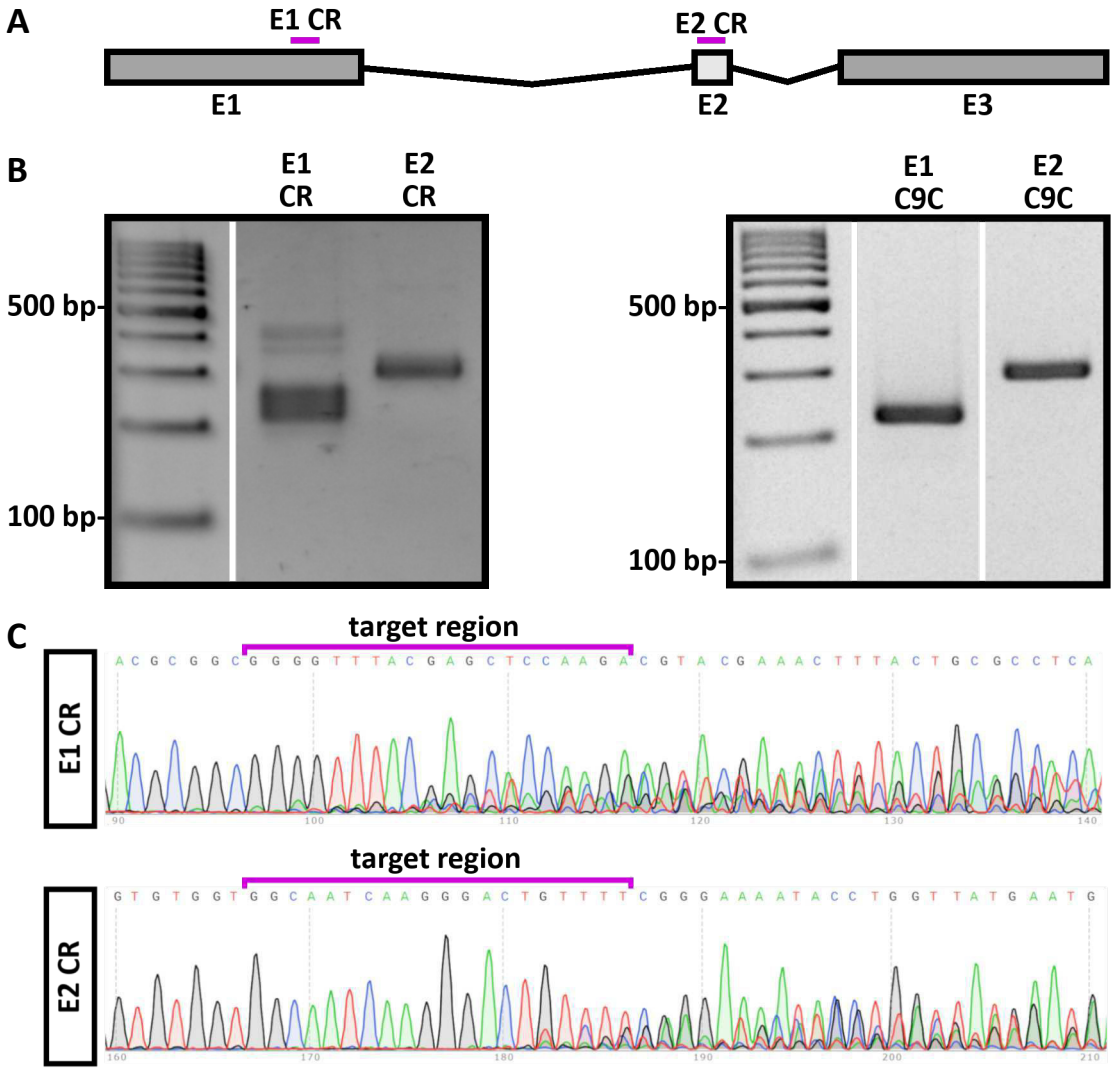


**Fig. S2. Validation of fgf3 CRISPR/Cas9. (A)** Scheme of *fgf3* gene with location of gRNA target region in exon 1 (E1 CR) and exon 2 (E2 CR) highlighted in magenta. **(B)** Examples of genotyping results from one 72 hpf embryo injected with both gRNAs together with Cas9 (left gel) and one 72 hpf control embryo injected with Cas9 only (C9C) (right gel). Note multiple bands for E1 CR and E2 CR gRNA in CRISPR/Cas9 injected embryo. The control embryo shows single wildtype bands (E1 C9C: 224 bp, E2 C9C: 289 bp) as a result of PCR amplification of E1 and E2 target regions. **(C)** DNA sequencing traces of genotyping PCR of CRISPR/Cas9 injected embryo (same specimen as for left gel in B) for E1 and E2 gRNA target regions revealed multiple traces due to indel mutations.

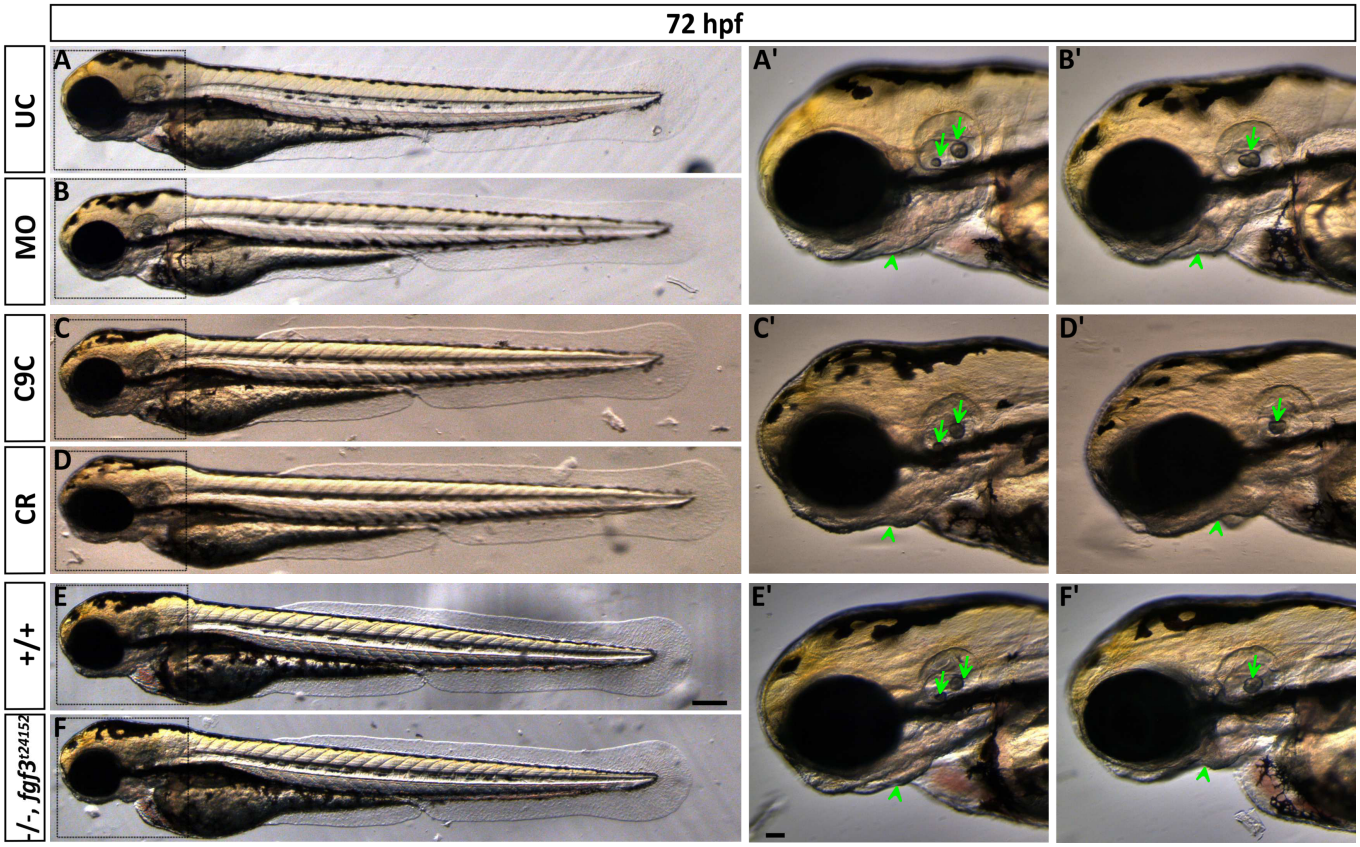


**Fig. S3. Live images showing morphology of 72 hpf embryos after *fgf3* impairment with characteristic ear and craniofacial malformations. (A,B)** Uninjected control (UC) and *fgf3* morpholino injected (MO) siblings. **(C,D)** Cas9 injected control (C9C) and *fgf3* CRISPR/Cas9 injected (CR) siblings. **(E,F)** Wildtype (+/+) and homozygous *fgf3t24152* mutant (-/-) siblings. Boxes indicate magnified area shown in **A'-F'**. After *fgf3* impairment the two otoliths fuse (arrow) and the lower jaw bones are malformed (arrow heads). Lateral views, anterior to the left. Scale bar in **E**, 100 µm; in **E'**, 50 µm.

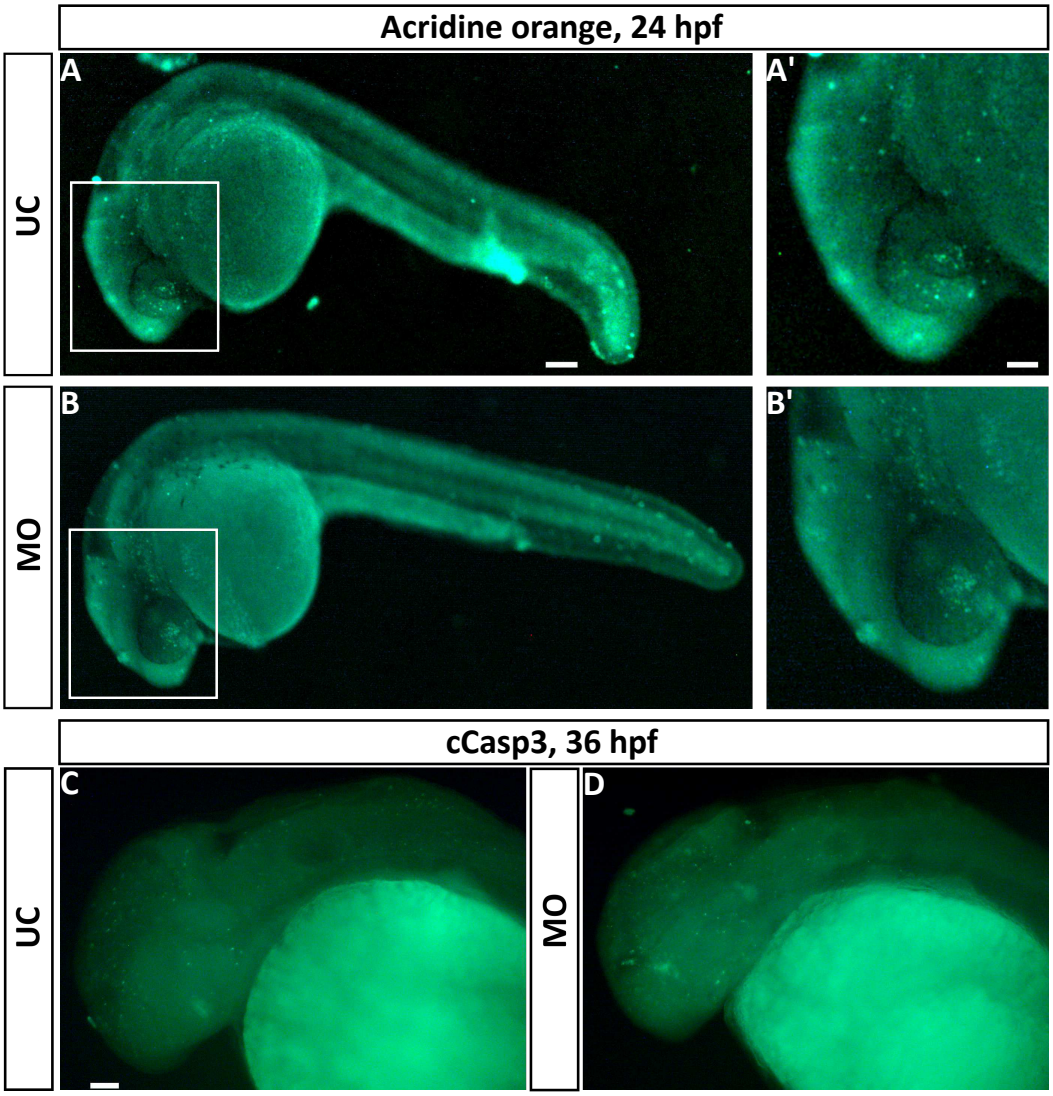


**Fig. S4. Fluorescence pictures showing cell death in *fgf3* morphants. (A,B)** Live images of acridine orange stained uninjected control (UC) and morphant (MO) siblings at 24 hpf. **A'** and **B'** are high magnifications of boxed areas in **A** and **B**. **(C,D)** Cleaved caspase 3 (cCasp3) immuno stained control and morphant siblings at 36 hpf. Lateral views, anterior to the left. Scale bar in **A**, 100 µm; in **A'** and **C** 50 µm.

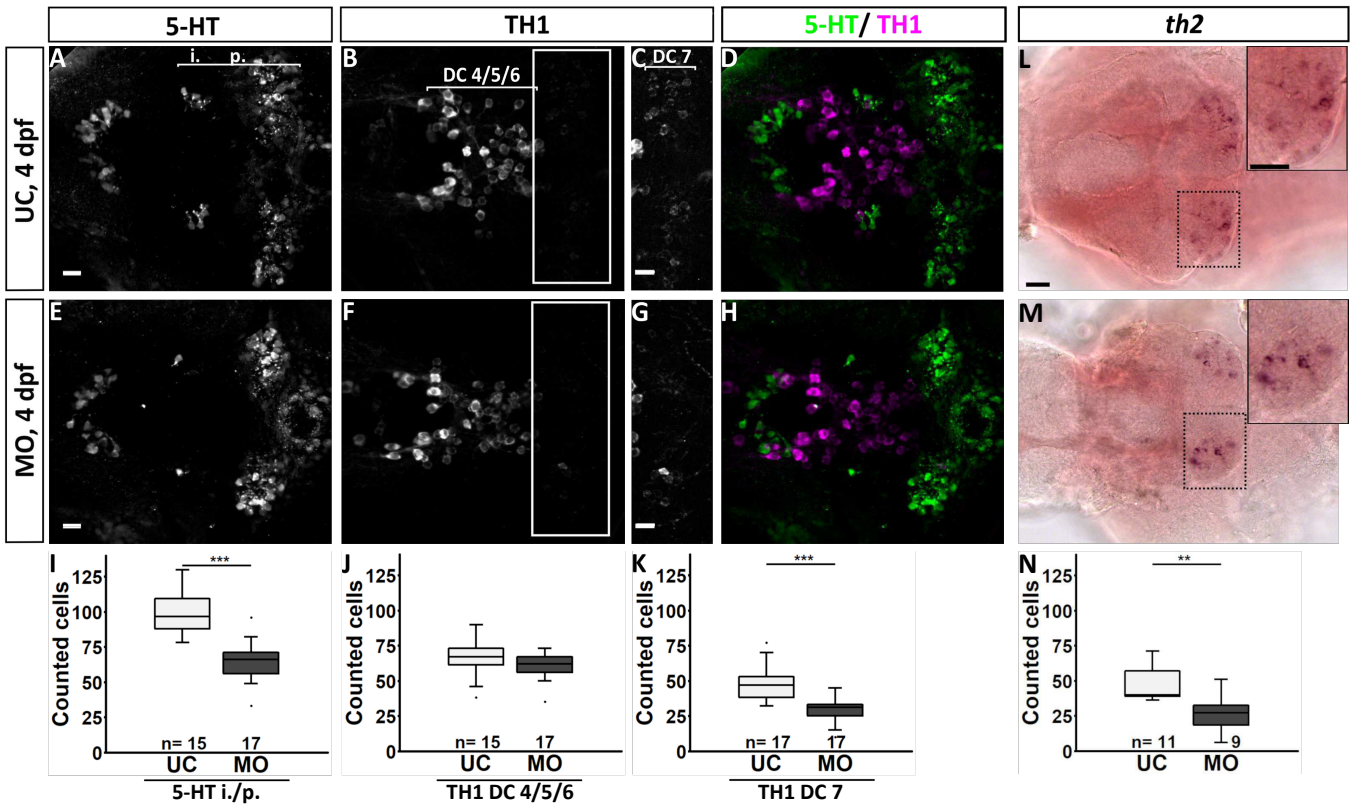


**Fig. S5. Quantification of the number of serotonergic cells in the intermediate (i.)/posterior (p.) clusters and of dopaminergic cells in the DC 4/5/6 and DC 7 clusters in the hypothalamus of *fgf3* morphants at 4 dpf. (A-H)** Confocal maximum intensity projections from uninjected control (UC) and morpholino injected (MO) siblings immuno stained for 5-HT (green) and TH1 (magenta) shown as single channels and merged. **C** and **G** show boxed areas in **B** and **F**, respectively, with adjusted brightness and contrast to reveal the faint TH1 immunoreactive cells of the DC 7 cluster. **(L, M)** Light microscopic pictures of *fgf3* morphants and uninjected control siblings processed for RNA *in situ* hybridisation for *th2* expressed by dopaminergic cells intermingled with TH1 positive cells in the DC 7 cluster. Insets show high magnifications of boxed areas. Ventral views, anterior to the left. Scale bars in **A,E,C,G**, 10 µm; in **L**, 30 µm. **(I-K, N)** Quantifications of 5-HT, TH1 and *th2* positive cells in control and morphant siblings. The number of serotonergic cells was counted in the i./p. clusters as indicated by the line in **A**. The number of dopaminergic (TH1 and *th2*) cells was counted in the DC 4/5/6 and DC 7 clusters as indicated by the lines in **B** and **C**, respectively. Tukey boxplots showing median, 25-75% percentile, IQR whiskers and outliers. n = number of analysed individuals.

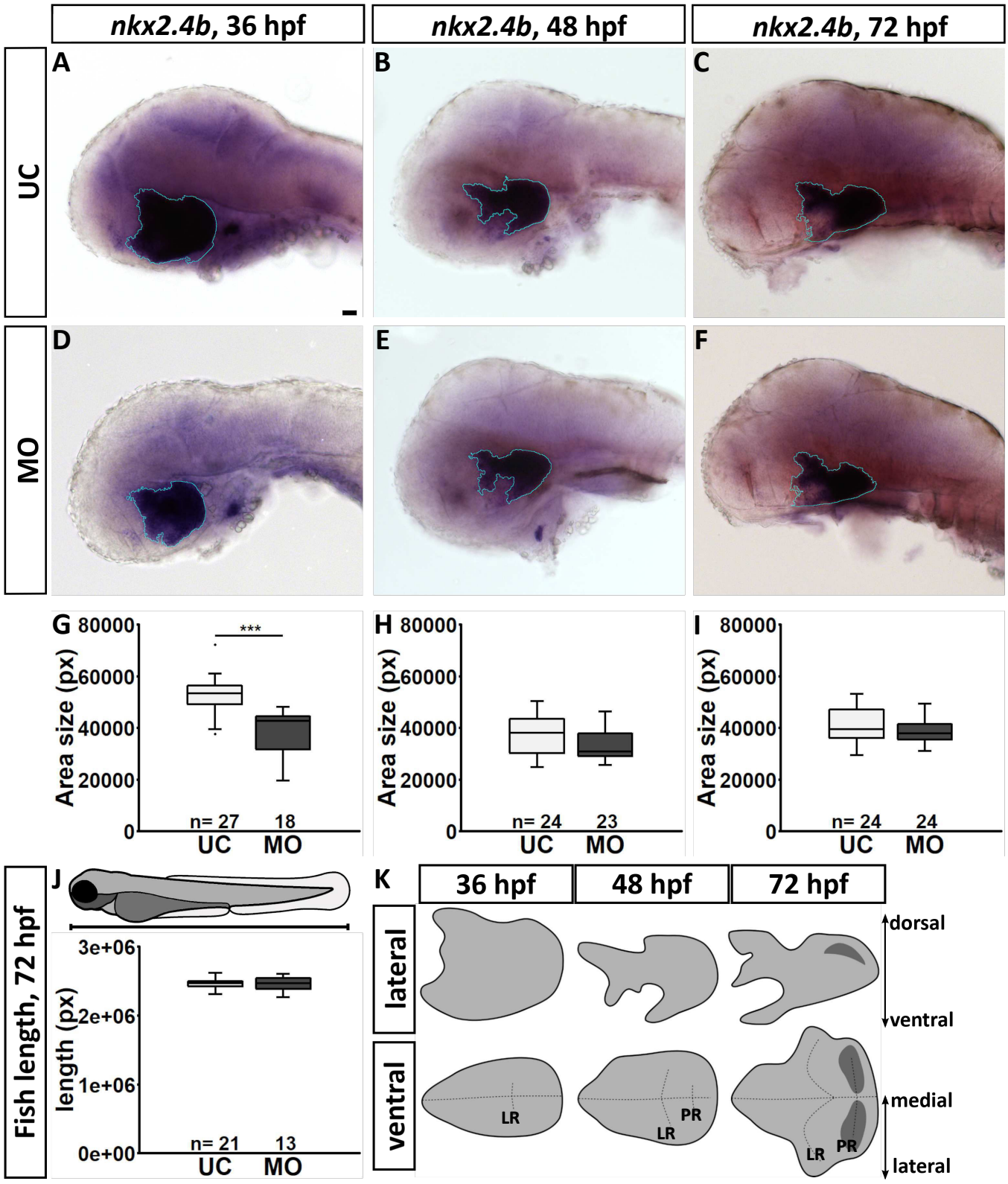


**Fig. S6. The shape of the hypothalamic *nkx2.4b* domain is altered in *fgf3* morphants. (A-F)** Light microscopic pictures showing expression of *nkx2.4b* in *fgf3* morphants (MO) and uninjected control siblings (UC) at 36, 48 and 72 hpf visualised by RNA *in situ* hybridisation. Outlines of semi-automated measurement of hypothalamic area are highlighted in blue. Lateral views, anterior to the left. Scale bar = 30 µm. **(G-I)** Area measurements (pixels) in *fgf3* morphants and control siblings of the *nkx2.4b* domain at 36, 48 and 72 hpf. **(J)** Total length measurements of *fgf3* morphants and control siblings at 72 hpf. Tukey boxplots showing median, 25-75% percentile, IQR whiskers and outliers. n= number of analysed individuals. **(K)** Scheme illustrating the lateral and ventral silhouette of the *nkx2.4b* expressing hypothalamic domain at 36, 48 and 72 hpf. Dark grey indicates location of monoaminergic populations around the posterior recess (PR). Dashed lines show hypothalamic ventricular system with the (LR) lateral recess and the PR.

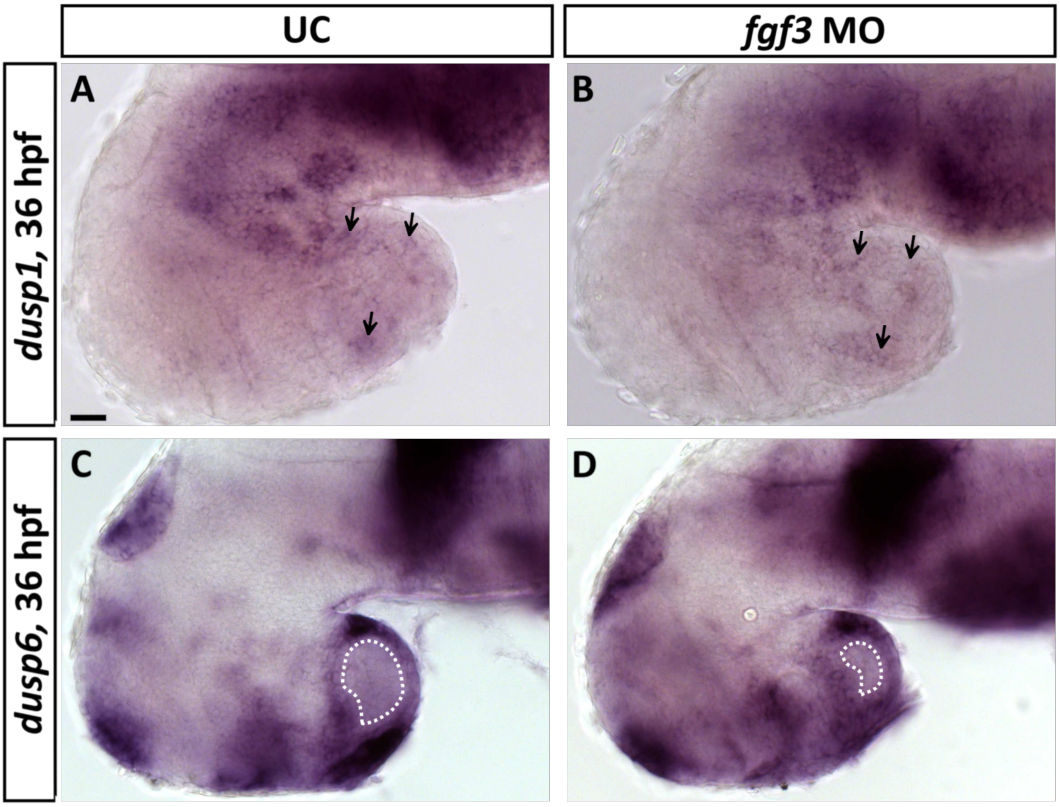


**Fig. S7. *fgf3* morphants exhibit mild alterations in expression of some Fgf-signalling targets. (A-D)** Light microscopic pictures of uninjected control (UC) and *fgf3* morphant (MO) siblings processed for RNA *in situ* hybridisation for *dusp1* and *dusp6* at 36 hpf. Notably, the hypothalamic *dusp1* expression is weaker in morphants compared to controls in hypothalamus (arrows) as well as in other brain regions (arrows). For *dusp6* the expression intensity is similar, but the size of the *dusp6* negative domain in posterior hypothalamus is reduced (dashed line). Lateral views, anterior to the left. Scale bar = 30 µm.

## References

**Devos, N., Deflorian, G., Biemar, F., Bortolussi, M., Martial, J. A., Peers, B., Argenton, F.** (2002). Differential expression of two somatostatin genes during zebrafish embryonic development. *Mechanisms of Development*. **1–2**, 133–137.

**Eaton, J. L., Holmqvist, B., Glasgow, E.** (2008). Ontogeny of vasotocin-expressing cells in zebrafish: selective requirement for the transcriptional regulators orthopedia and single-minded 1 in the preoptic area. *Dev. Dyn.* **4**, 995–1005.

**Kiefer, P., Strähle, U., Dickson, C.** (1996). The zebrafish Fgf-3 gene: cDNA sequence, transcript structure and genomic organization. *Gene*. **2**, 211–215.

**Münchberg, S. R., Ober, E. A., Steinbeisser, H.** (1999). Expression of the Ets transcription factors erm and pea3 in early zebrafish development. *Mechanisms of Development*. **2**, 233–236.

**Rohr, K. B., Concha, M. L.** (2000). Expression of nk2.1a during early development of the thyroid gland in zebrafish. *Mechanisms of Development*. **1-2**, 267–270.

**Tsang, M., Maegawa, S., Kiang, A., Habas, R., Weinberg, E., Dawid, I. B.** (2004). A role for MKP3 in axial patterning of the zebrafish embryo. *Development*. **12**, 2769–2779.

**Unger, J. L., Glasgow, E.** (2003). Expression of isotocin-neurophysin mRNA in developing zebrafish. *Gene Expression Patterns*. **1**, 105–108.

**Yamamoto, K., Ruuskanen, J. O., Wullimann, M. F., Vernier, P.** (2010). Two tyrosine hydroxylase genes in vertebrates New dopaminergic territories revealed in the zebrafish brain. *Mol Cell Neurosci*. **4**, 394–402.